INDOOR RADON MEASUREMENTS IN THE ABANT IZZET BAYSAL UNIVERSITY CAMPUS

by

ŞEYMA ATİK

THESIS SUBMITTED TO
THE GRADUATE SCHOOL OF NATURAL AND APPLIED SCIENCES
OF
THE ABANT İZZET BAYSAL UNIVERSITY
IN PARTIAL FULFILLMENT OF THE REQUIREMENTS FOR THE
DEGREE OF
MASTER OF SCIENCE
IN
THE DEPARTMENT OF PHYSICS

JANUARY 2014

Approval of the Graduate School of Natural Sciences

Prof. Dr. Yaşar Dürüst

Director

I certify that this thesis satisfies all the requirements as a thesis for the degree of Master of Science.

Prof. Dr. İbrahim Belenli

Head of Physics Department

This is to certify that we have read this thesis and that in our opinion it is fully adequate, in scope and quality as a thesis for the degree of Master of Science.

Assoc. Prof. Dr. Hakan Yetiş

Co-Supervisor

Prof. Dr. Haluk Denizli

Supervisor

Examining Committee Members

1. Prof. Dr. Haluk DENİZLİ .....

2. Assoc. Prof. Dr. Hakan YETİŞ .....

3. Prof. Dr. Fatih EVRENDİLEK .....

4. Assoc. Prof. Dr. Cihan PARLAK .....

5. Assoc. Prof. Dr. Hünkar KAYHAN .....

To my sweet family members:

My parents, sister, brother and my grandparents

ACKNOWLEDGEMENTS

First of all, praises to almighty Allah because I have never alone, I feel always a power with me all along this thesis and master career.

I am deeply grateful to my supervisor Prof. Dr. Haluk Denizli for his guidance and encouragement during the entire period of my studies. I am thankful to my co-supervisor Assoc. Prof. Dr. Hakan Yetiş for his valuable helps and advices to complete this research work. I am especially thankful to Prof. Dr. Fatih Evrendilek for his academic experience about statistics and helps for the learning of modelling.

A special thanks to Ali Yılmaz for always being with me from undergraduate and his advices for all kinds of problem when I came face to face. I am grateful to the teachers, staff and my colleagues for helping me to the installation and data acquisition in the offices and commisaries of faculties.

I would like to thank to Scientific Research Projects Unit (BAP) for supporting this work under the grant number: BAP - 2011.03.02.425, by Abant Izzet Baysal University.

Last but not the least I am heartily grateful to my family members who supported and encouraged me a lot during my studies, their prayers and good wishes always accompanied me.

ABSTRACT

INDOOR RADON MEASUREMENTS IN THE ABANT IZZET BAYSAL UNIVERSITY CAMPUS

Atik, Şeyma

Master of Science, Department of Physics

Supervisor: Prof. Dr. Haluk Denizli

Co-Supervisor: Assoc. Prof. Dr. Hakan Yetiş

January 2014, 66 pages

Indoor radon concentration was measured by using AlphaGuard Radon Monitor and short term Electret Chambers from May 2012 to May 2013. Measurements followed a randomized and repeated pattern of experimental design. All the measurements were carried out at five faculty buildings of AIBU. For instance at the Faculty of Arts and Science where we used only AlphaGuard monitor to figure out the dependence of the radon concentration on the floor level and aspect directions (south vs north). Following the Tukey's multiple comparisons, one-way and two-way Analysis of Variance (ANOVA), General Linear Model (GLM) and Regression Analysis were performed. The Best Artificial Neural Networks (ANNs) emulating indoor radon levels were selected as a function of air temperature, air pressure, relative humidity, air temperature by relative humidity interaction, local time, location, month, floor and aspect. Out of 27 ANNs, MLP-2-B-L and MLP with PCA (for both AlphaGUARD and ST Chambers) performed best and could be contributing to 96.7%, 59.1% and 87.6% of variations in spatio-temporal dynamics of indoor radon levels as a function of floor level and aspect or location

respectively, in addition to air temperature, air pressure, relative humidity, air temperature by relative humidity interaction, time and location, month, location by month interaction. The mean indoor radon levels stay below the reference level to minimise health risks due to indoor radon exposure.

Key Words: Indoor Radon, Neural Networks, Spatio-Temporal Dynamics, Modelling

ÖZET

ABANT İZZET BAYSAL ÜNİVERSİTESİ BİNA İÇİ RADON GAZI ÖLÇÜMÜ

Atik, Şeyma

Yüksek Lisans, Fizik Bölümü

Tez Danışmanı: Prof. Dr. Haluk Denizli

Ortak Tez Danışmanı: Doç. Dr. Hakan Yetiş

Ocak 2014, 66 sayfa

Mayıs 2012'den ve Mayıs 2013'e kadar bina içi radon konsantrasyonu, AlphaGUARD P30 radon detektörü ve kısa süreli Elektret Odaları kullanılarak ölçülmüştür. Ölçümlerde rastgele ve tekrarlayan bir deney planı izlenmiştir. Tüm ölçümler Abant İzzet Baysal Üniversitesi'nin 5 fakültesinde gerçekleştirilmiştir. Örneğin Fen Edebiyat Fakültesinde yalnızca AlphaGUARD P30 radon detektörü kullanılarak radon seviyesinin kat yüksekliğine ve cephe yönüne bağımlılığı hesaplanmıştır. Tukey'in çoklu karşılaştırma testini izleyen tek-yönlü ve iki-yönlü Varyans Analizi (ANOVA), Genel Lineer Model (GLM) ve Regresyon Analizleri yapıl-mıştır. En iyi Yapay Sinir Ağları (YSA) benzetimi için bina içi radon seviyeleri hava sıcaklığına, hava basıncına, bağıl neme, hava sıcaklığı ve bağıl nem etkileşimine, yerel zamana, konuma, aya, kat yüksekliğine ve cephe yönününe bağlı bir fonksiyon olarak seçilmiştir. 27 YSA'nın dışında, en iyi performanslar MLP-2-B-L ve iki PCA'lı MLP (AlphaGUARD ve ST Chamber için) olup, uzaysal-zamansal dinamiklerin değişimi sırasıyla kat yüksekliği ve cephe yönü veya konum, bunlara ek olarak hava sıcaklığı, hava basıncı, bağıl nem, hava sıcaklığı ve bağıl

nem etkileşimi, zaman ve konuma bağlı bir fonksiyon olan bina içi radon seviyelerine %96.7, %59.1 ve %87.6 kadar katkıda bulunmaktadır. Tüm ortalama radon konsantrasyonları, bina içi radona maruz kalmaktan dolayı sağlığımız için tehdit oluşturan en düşük seviyenin altındadır.

Anahtar Kelimeler: Bina İçi Radon, Sinir Ağları, Uzay-Zamansal Dinamikler, Modelleme

TABLE OF CONTENTS

LIST OF FIGURES

LIST OF TABLES

CHAPTER 1

INTRODUCTION

All living beings are continuously exposed to the natural external and internal sources of radiation. Cosmic and terrestrial gamma rays are some natural external sources. Soil, rocks, water, food, medical materials and building materials due to radionuclides in the nature are natural internal sources. The worldwide average background dose for a human being, depending on the physical and geological features of the place, is about 2.8 mSv per year [1]. About 82% of the environmental radiation results from natural sources and a very important contribution to inhalation exposure is made by radon and its decay products which is about 1.2 mSv of the annual equivalent dose. Other part of internal radiation is about 0.4 mSv which results from medical radiation. The dose from external sources is approximately 0.9 mSv, shared as 0.4 mSv due to the cosmic radiation and 0.5 mSv due to the terrestrial gamma radiation. The remainder part of equivalent dose is 0.3 mSv which originates from ingestion of Potassium-40 (^{40}K) in foods [2].

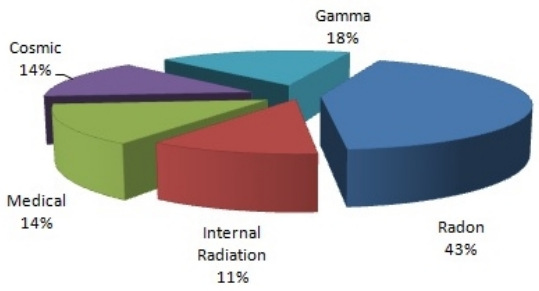

Figure 1.1: The radiation percentages of external and internal sources.

Radon is a naturally occurring radioactive gas released in rock, soil and water. According to EPA, radon gas is odorless and invisible and the only way to know

is to test for it. Breathing radon can increase the risk of lung cancer. In the 19th century, about 75% of the miners died from lung cancer. After the identification of radon by Marie and Pierre Curie, the first measurements in the mines were made in 1901. After more precise measurements, a correlation between radon exposure and lung cancer was suggested in the 1920s. This hypothesis was confirmed in 1940 [3].

In the 1950s, the first measurement on indoor radon level was performed by Hultqvist in 300 dwellings located at four different cities in Sweden [4]. Furthermore this exploratory application involved measurements of gamma radiation in about 1,000 dwellings in Sweden. According to this study of Rolf Sievert, while some houses maden from alum-shale concrete were having high radon levels, a few dwellings built from other materials as wood, brick had low radon concentration. The levels were found in the range of 20 to 500 $Bq{\cdot}m^{-3}$. After Hultqvist's investigations, the radon measurements were interrupted in Sweden. At the end of the 1960's and the beginning of the 1970's measurements in dwellings were tackled again partly as a result of the reports on the correlation between lung cancer among miners and radon exposure.In the 1970's the Swedish Radiation Protection Institute (SSI) launched a rather extensive measurement program on radon in dwellings. The current interest was mainly focused on-dwellings built from lightweight concrete based on alum shale. In 1979, a sample survey related with statistical significance of radon levels in Swedish dwellings was began [5].

In the same period several measurements were made on indoor and outdoor radon all over the world. Many countries performed indoor and outdoor radon measurements and designated their radon exhalation rates. In particular, the United States and Europe gave great importance to such studies. United States Enviromental Protection Agency (EPA) created a radon map for 3,141 counties in the U.S. with the help of these measurements [6]. Three concentration zones were constituted by EPA. The highest potential level is named red zone which

has predicted average indoor radon level greater than 4pCi/L, moderate potential level is named orange zone which has average indoor radon level between 2 and 4 pCi/L and the yellow zone has average indoor radon level less than 2 pCi/L which is low potential zone. Many other countries determine their limit values for indoor radon concentration that is a changeable value from one country to another one. This change is related with the geological structure, climate condition, soil structure, location or altitude and many more factor. Indoor radon concentration is also related with building materials, location of building, indoor air quality or ventilation.

Table 1.1: The mean radon concentrations in dwellings [7]

Country	Concentration ($Bq \cdot m^{-3}$)	Country	Concentration ($Bq \cdot m^{-3}$)
U.S.	46	France	62
Germany	50	Hungary	107
India	57	Egypt	9
Argentina	37	Netherlands	23
Australia	37	Norway	73
United Kingdom	20	Poland	41
Turkey	52	Italy	75
China	24	Japan	16
Czech Republic	140	Sweden	108
Canada	34	Greece	73
Armenia	104	Portugal	62
Syria	44	Iran	82

Table 1.1 shows the estimated average of indoor radon in dwellings for many countries, reported by Yücel. The maximum average indoor radon concentration is 140 $Bq \cdot m^{-3}$ in Czech Republic and the minimum value is 9 $Bq \cdot m^{-3}$ in Egypt. Furthermore the limit values of indoor radon concentration are determined across the globe. The permissible concentrations of radon for various countries and international organizations are given in Table 1.2.

Radon contributes up to 40% of the dose of ionizing radiation received by the population. Studies performed on cohorts of uranium miners clearly showed the a linear relation between exposure to radon and risk of lung cancer. This relation

Table 1.2: The indoor radon concentration limit values [7]

Country	Concentration ($Bq \cdot m^{-3}$)	Country	Concentration ($Bq \cdot m^{-3}$)
U.S.	150	United Kingdom	200
Australia	250	Germany	250
Luxembourg	250	China	200
India	150	Rusia	200
Danmark	400	Ireland	200
Turkey	400	Sweden	200
France	400	Canada	800
Norway	200	AB	400
ICRP	400	WHO	100

is dependent on the age, time since exposure and duration of exposure. Pooled analyses of key studies in China, Europe and North America have confirmed that radon in homes contributes substantially to the occurrence of lung cancers worldwide. On the basis of these studies, the International Agency for Research on Cancer (IARC) and the US National Toxicology Program have classified radon as a human carcinogen. According to EPA, radon is the most important reason of lung cancer among non-smokers. EPA estimates that radon causes more than 20,000 deaths from lung cancer each year in the U.S. Radon has been classified as a known human carcinogen and has been recognized as a significant health problem by groups such as the Centers for Disease Control, the American Lung Association, the American Medical Association, and the American Public Health Association.

As individuals spend more than 90% of their time indoors, the exposure to radon becomes a significant problem. Most of the radon in indoor air is due to the penetration of radon gas in the ground through cracks and gaps into the buildings and generally being in the basement of the buildings. The basements are important because they are the connection point of the building with soil. Also radon diffuses from soil or rocks and it comes to the indoor of the building. The measurement of indoor radon concentration in the buildings or non-ventilated enclosed spaces has significant importance for human health.

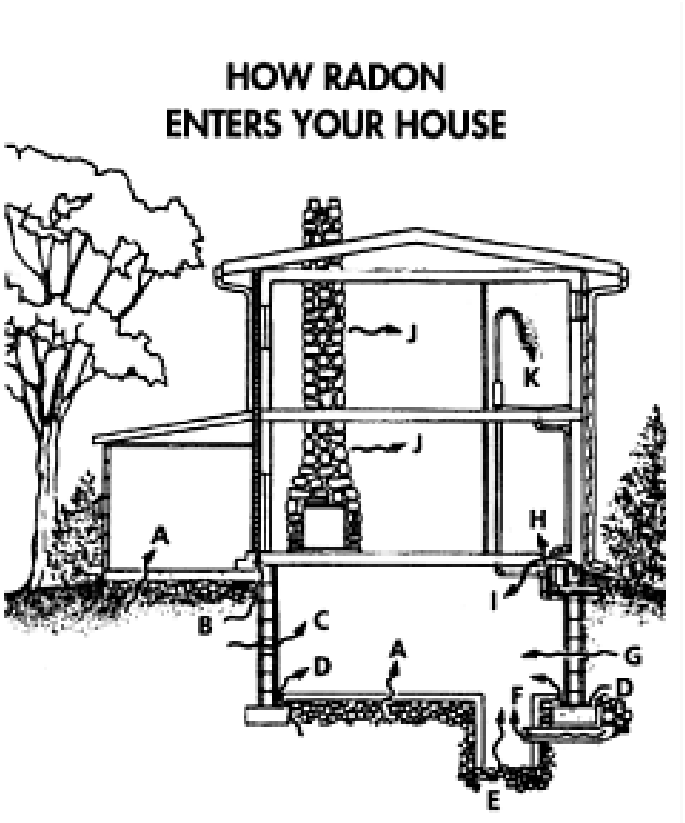

Figure 1.2: How radon enters the homes [8]

Radon gas can enter a home from the soil through cracks in concrete floors and walls, floor drains, sump pumps, construction joints, and tiny cracks or pores in hollow-block walls. Radon levels are generally highest in basements and ground floor rooms that are in contact with the soil. Factors such as the design, construction, and ventilation of the home affect the pathways and sources that can draw radon indoors. Another source of radon indoors may be air released by well water during showering and other household activities. Compared to radon entering the home through soil, radon entering the home through water will in most cases be a small source of risk.

The aim of the present study is to see the seasonal effects on radon concentration and to related two different types of detector with each other. Radon is a well-known problem for human health so; measurements of indoor radon concentration is important for commissaries of faculties. Another importance of radon

is related with earthquake in literature. The campus area is near to the North Anatolian Fault zone and indoor radon measurements have been never made in Bolu, especially in the campus site of Abant Izzet Baysal University.

This thesis has been divided into six chapters.

- Chapter 1 gives an overview of radon. The literature about radon measurements and the relationship between radon and lung cancer are briefly described. The indoor radon concentration levels for many countries are given with numerical values.

- Chapter 2 gives the brief history for discovery of radioactivity, types of radiation and its decay properties. Radon sources in nature and its general properties are described.

- In chapter 3, the current detector types for the present study and the properties of them are given. This chapter deals with the measurement of indoor radon levels in faculties. The measurements were performed in commissaries and a specific building throughout the year in twelve cycles to cover all the seasons.

- Chapter 4 briefly gives the statistical methods mentioned in this thesis. Minitab statistical package and NeuroSolutions are the most important within them.

- The studies regarding measurement of seasonal variation of indoor radon levels and relation between two types detector are presented in chapter 5. The results of statistical analyses for indoor radon concentrations, ambient air conditions, location and time are also presented. The tables and figures are given in the result part. Assessment of lung cancer risk using measured indoor radon levels have been dealt with in chapter 5.

- Chapter 6 concludes the present work, general discussion of the main results in this chapter.

CHAPTER 2

RADIATION AND RADIOACTIVITY

In late 1895 the X-ray was discovered by Wilhelm Conrad Roentgen. He was working with a cathode ray tube. He vacuumed the tube of all air then filled it with a special gas, and passed a high electric voltage through it. When he did this process the tube produced a fluorescent glow. He twined around the tube with a black paper, and found that a green colored fluorescent light. Thereby a new ray or invisible light discovered by Roentgen, named the new ray X-ray, because 'X' is used to indicated the unknown quantity in the mathematics [9]. With this discovery, many scientist would think about whether all fluorescent materials give X-ray or not. Many of physicochemisist started investigations but the trials gave negative results on zinc sulphide and calsium sulphide. Henry Becquerel exposed potassium uranyl sulfate to sunlight and then placed it on photographic plates wrapped in black paper, believing that the uranium absorbed the Sun's energy and then emitted it as X-rays. This hypothesis was disproved because the weather was cloudy during the experiment in Paris. For some reason, Becquerel decided to develop his photographic plates anyway. Proving that, the images were more clear and strong without any external source such as sun, so uranium emitted the radiation. In this way, the radioactivity was discovered in 1896 by Henry Becquerel [10].

The radioactivity means that an unstable atom which has excess energy emits a particle or ray and it forms a different stable atom. This process is called as radioactivity or radiactive decay and the emitted particle or ray called as radiation. In the following section, well known types of radiation are presented.

2.1 Types of Radiation

Radiation is classified into two categories which are known as ionizing and non-ionizing radiation. These categories denote that energy and hazardous to body.

2.1.1 Ionizing Radiation

Ionizing radiation has the ability to remove electrons from atoms and creates ions. The result of ionization is the production of negatively charged free electrons and positively charged ionized atoms. There are four types of ionizing radiation involved that can be classified into two groups: first photons, such as gamma and x-rays, and second particles, such as beta particles; positrons or electrons, third alpha particles; similar to helium nuclei, 2 protons and 2 neutrons, and last neutrons particles with zero charge. Photons are electromagnetic radiation having energy, but no mass or charge; whereas particles have typically mass and charge as well as energy. Neutrons have mass and energy, but no charge, and are typically produced in the laboratories, such as cyclotrons. All types of ionizing radiation can remove electrons, but interact with matter in different ways.

Particles are more highly ionizing; excitation and ionization are the primary interaction with matter, and potential for ionization increases as mass and charge increase. The range in tissue (depth to which the radiation may penetrate) for particles decreases as mass and charge increase. Photons, because they have no mass or charge, are less ionizing but more penetrating in matter.

Ionized atoms, regardless of how they were formed, are much more active chemically than neutral atoms. These chemically active ions can form compounds that interfere with the process of cell division and metabolism. Also, reactive ions can cause a cascade of chemical changes in the tissue. The degree of damage suffered by an individual exposed to ionizing radiation is a function of several factors: type of radiation involved, chemical form of the radiation, intensity of

the radiation flux (related to the amount of radiation and distance from the source), energy, and duration of exposure [11].

2.1.2 Nonionizing Radiation

Nonionizing radiation originates from various sources: Natural origin (such as sunlight or lightning discharges etc.) and man made (seen in wireless communications, industrial, scientific and medical applications). Nonionizing spectrum is divided into two main regions; optical radiations and electromagnetic fields [12].

2.1.2.1 Optical Radiations

The optical radiations are centred around visible light; those with higher energies are termed UV radiation and those with lower energies infrared (IR) radiation.

Sources of UV radiation are the sun, arc welding, oxy-gas welding, sun lamps, lasers (UV), sterilization (germicidal) lamps, low pressure gas discharge lamps, high pressure discharge lamps. Sources of IR radiation are from hot processes such as steelmaking, glassmaking, welding, and also lasers (IR). The application of laser as a coherent light source is increasing rapidly.

Medical applications include UV and neonatal phototherapy, surgical and therapy lasers, physiotherapy heat lamps [12].

2.1.2.2 Electromagnetic Fields

Microwaves are used in telecommunications, radar/satellite links, mobile phones, microwave ovens, TV transmitters. RF is used in radio communications, visual display units, television sets. Extremely low-frequency (ELF) electric and magnetic fields (EMFs) surround electrical machinery, home appliances, electric wiring, and high-voltage electrical transmission lines and transformers.

Medical applications include: microwave hyperthermia, therapeutic and surgical diathermy, and magnetic resonance imaging (MRI) [12].

2.2 The Basic Concepts of Radioactive Decay

The radioactive decays of naturally occurring minerals containing uranium and thorium are in large part responsible for the birth of the study of nuclear physics. These decays have half-lives that are of the order of the age of the Earth suggesting that the materials are survivors of an early period in the creation of matter by aggregation of nucleons: the shorter lived nuclei have long since decayed away and we observe today the remaining long-lived decays [13]. In the following, basic subtitle of radioactive decay will discoursed.

2.2.1 The Radioactive Decay Law

Radioactive decay is a random process. As such, one cannot state with certainty when an unstable nuclide will decay. The probability that an atom will decay during the time dt is given by λdt where λ is the constant of proportionality known as the decay constant. In a system where there are $N(0)$ atoms present initially, the number of atoms decaying in time dt is given by $-dN = \lambda N dt$. In the limit of very small time intervals, this can be expressed as

$$\frac{dN}{dt} = -\lambda N \tag{2.1}$$

Integration with respect to time gives the number of atoms present at any time t [14].

$$N(t) = N(0)e^{-\lambda t} \tag{2.2}$$

2.2.2 Activity

The activity or strength of a radiactive sample is defined as the mean number of decay processes it undergoes per unit time. This is an extrinsic quantity which depends on the amount of source material contained in the sample (the larger sample the greater the total number of decays) [15].

The number of decays per unit time interval, i.e. the activity A, is defined by

$$A = -\frac{dN}{dt} = \lambda N \tag{2.3}$$

2.2.3 Half-life and Mean life Time

The half-life, $t_{\frac{1}{2}}$, is used to denote the time at which the number of atoms has decreased to half the initial value, i.e. $\frac{1}{2} = e^{-\lambda t_{\frac{1}{2}}}$. Hence the half-life is related to the decay constant through the relation [14].

$$t_{\frac{1}{2}} = \frac{In2}{\lambda} \approx \frac{0.693}{\lambda} \tag{2.4}$$

Another useful time scale for describing decays is the average or mean life time of a radioactive material (τ) which is defined as the average time that a nucleus is likely to survive before it decays, and it can be shown that it relates to the decay constant (λ) in the following way [16].

$$\tau = \frac{1}{\lambda} \tag{2.5}$$

2.3 Radiation Decay Types and Properties

There are generally three types of radiation associated with radioactive decay which alpha decay, beta decay and gamma decay.

2.3.1 Alpha Particles

The spontaneous emission of an alpha particle can be represented by the following process:

$$ {}^{A}_{Z}X_{N} \rightarrow {}^{A-4}_{Z-2}X'_{N-2} + \alpha \tag{2.6} $$

Alpha particles are a type of ionizing radiation ejected by the nuclei of some unstable atoms which have symbol as α. An helium nucleus (${}^{4}_{2}He$) which have two neutrons and two protons. Where X and X' are the initial and final nuclei, A is the total mass number, N is the number of neutrons and Z is the number of protons in nucleus [13]. Alpha particles emitted from heavy nucleus as uranium, polonium, thorium, radium which neutron numbers are much more than protons numbers. Alpha particles are positively charged due to two protons its structure and have a heavy mass due to its neutrons and protons. Alpha particles have a velocity in air of approximately one-twentieth the speed of light, depending upon the individual particle's energy. While they passing from a matter, they can easily absorbed since their trajectories are short.

$$ {}^{226}_{88}Ra \rightarrow {}^{222}_{86}Rn + {}^{4}_{2}He \tag{2.7} $$

An important example on this type of decay is the decay of Radium-226 into Radon-222 as shown in equation (2.7). Uranium (^{238}U), Radium (^{226}Ra) and Radon (^{222}Rn) are typical alpha particle emitters.

2.3.2 Beta Particles

The most basic β decay process is the conversion of a proton to a neutron or of neutron into a proton. In a nucleus β decay changes both Z and N by one unit: $Z \rightarrow Z \pm 1$, $N \rightarrow N \pm 1$ so that $A = Z + N$ remains constant. Beta particles can have either a negative charge or a positive charge and they have

the same very small mass (1/2000 the mass of a neutron) regardless of charge. Beta particles can penetrate farther than alpha particles (its penetration distance depends upon the energy of beta particle and material used); however, they can be stopped fairly easily by a sheet of aluminum.

$$\begin{aligned} n &\rightarrow p + e^- \qquad \beta^- decay \\ p &\rightarrow n + e^+ \qquad \beta^+ decay \\ p + e^- &\rightarrow n \qquad electron \quad capture \quad (\epsilon) \end{aligned}$$

The process is known as negative β decay or negatron decay and involves the creation and emission of an ordinary electron. The second process is positive β decay or positron decay, in which a positively charged electron is emitted. In the third process an atomic electron that strays too close to the nucleus is swallowed, allowing the conversion of a proton to a neutron. In all three processes, yet another particle called a neutrino is also emitted, but since the neutrino has no electric charge, its inclusion in the decay process does not affect the identity of the other final particles [13].

2.3.3 Gamma Particles

Gamma rays are electromagnetic waves emitted by radioactive nuclei (such as ^{60}Co and ^{137}Cs) and during certain nuclear reactions. High energy gamma rays are a component of cosmic rays that enter the Earth's atmosphere from space. They have wavelengths ranging from approximately $10^{-10}m$ to less than $10^{-14}m$. They are highly penetrating and produce serious damage when absorbed by living tissues. Consequently, those working near such dangerous radiation must be protected with heavily absorbing materials, such as thick layers of lead [17].

Radioactive γ emission is analogous to the emission of atomic radiations such as optical or x-ray transitions. An excited state decays to a lower excited or possibly the ground state by the emission of a photon of γ radiation of energy

equal to the difference in energy between nuclear states [13]. Emission of a gamma ray from an excited nuclear state typically requires only 10^{-12} seconds, and is thus nearly instantaneous [18].

2.4 Radiation Units

Two types of units are used for radiation, units of activity and units of exposure (dose). Units of activity quantify the amount of radiation emitted by a given radiation source. Units of exposure quantify the amount of radiation absorbed or deposited in a specific material by a radiation source [11].

The number of disintegrations, or decay events, or nuclear transformations, in a sample per unit time is its activity A. Two common informal units are disintegrations per second and disintegrations per minute.

The US unit of activity is the Curie (Ci). One Curie is $2.2{*}10^{12}$ disintegrations per minute, or $3.7 * 10^{10}$ disintegrations per second. Common multiples are the millicurie and microcurie. The SI unit of activity is the Becquerel (Bq). One Becquerel is 1 disintegration per second [19].

$$\begin{aligned} 1 \quad & Ci = 3.7 * 10^{10} \quad Bq \\ 1 \quad & Becquerel = 2.7 * 10^{-11} \quad Curie \end{aligned} \tag{2.8}$$

The Roentgen (R) is a measure of exposure to X-ray or gamma ray radiation. One roentgen is that amount of X-ray or gamma radiation that will deposit enough energy to strip about two billion electrons from their orbits (called one electrostatic unit) in one cubic centimeter of dry air. The roentgen technically applies only to ionization in dry air from X-ray or gamma radiation and does not apply to damage to body tissues [20].

The Radiation Absorbed Dose (RAD) is a measure of the absorbed dose (energy deposited) in a material. One RAD is the deposition of one hundred ergs of energy in one gram of any material due to the ionization from any type of radi-

ation. One erg of energy is equal to about one ten billionth of a BTU, or about one ten millionth of a watt. The Gray is the SI unit of absorbed dose. A Gray is equal to 0.1 Joule of energy deposited in one kilogram of matter. Therefore, one RAD is equivalent to 1/100 of a gray, and one gray is equal to 100 RADs.

The REM is based on the biological damage caused by ionization in human body tissue. It is a term for dose equivalence and equals the biological damage that would be caused by one RAD of dose. The REM accounts for the fact that not all types of radiation are equally effective in producing biological change or damage. That is, the damage from one rad deposited by beta radiation is less than that caused by one rad of alpha radiation. The sievert is the SI unit of dose equivalent. In the same way that converting from the absorbed dose (RAD) to the dose equivalent (REM) involved the use of quality factors, the conversion of grays to sieverts also uses quality factors. One rem equals 1/100th of a sievert, and one sievert equals 100 rems [20].

$$\begin{aligned} 1 \quad RAD &= 0.01 \quad Gray \\ 1 \quad REM &= 0.01 \quad Sievert \end{aligned} \tag{2.9}$$

2.5 Radon and Its Progeny

Radon was discovered in 1900 by Friedrich Ernst Dorn which is a radioactive, colorless, odorless, tastless noble gas, occurring naturally as the decay product of uranium or thorium, and have 86 atomic number. It's most common and stable form, Radon-222, has a half-life of 3.8 days, and will eventually decay in to Lead-206. Its melting and evaporation temperature is -71°C and -61.8°C, respectively. Radon forms a monatomic gas with a density of 9.73 kgm^{-3} at standard temperature and pressure, about 8 times bigger than the density of the Earth's atmosphere at sea level. Radon is one of the densest gases at room temperature and is the densest of the noble gases [21].

Table 2.1: Decay series of Uranium (^{238}U)

Isotope	Half life	Decay
^{238}U	$4.49 * 10^9 y$	α
^{234}Th	$24.1d$	β^-
^{234}Pa	$1.17min$	β^-
^{234}U	$2.48 * 10^5 y$	α
^{230}Th	$7.7 * 10^4 y$	α
^{226}Ra	$1600y$	α
^{222}Rn	$3.82d$	α
^{218}Po	$3.05min$	α
^{214}Pb	$26.8min$	β^-
^{214}Bi	$19.8min$	β^-
^{214}Po	$162\mu s$	α
^{210}Pb	$22.3y$	β^-
^{210}Bi	$5.01d$	β^-
^{210}Po	$138.4d$	α
^{206}Pb	stable	-

The three naturally occurring radioactive isotopes of radon are; ^{222}Rn radon is a decay product of the uranium series in Table 2.1, ^{220}Rn thoron is derived from thorium series in Table 2.3 and ^{219}Rn actinon is a decay product of actinium series in Table 2.2 . Thorium and uranium are the two most common radioactive elements on earth; they have been around since the earth was formed. Their naturally occurring isotopes have very long half-lives, on the order of billions of years. Thorium and uranium, their decay product radium, and its decay product radon, will therefore continue to occur for tens of millions of years at almost the same concentrations as they do now [22].

The relative importance of the three radon isotopes depends on their mean lives and relative abundance. The mean lives of ^{222}Rn, ^{220}Rn and ^{219}Rn are $5.51d$, $80.2s$, and $5.71s$ respectively. The natural ratio of $^{235}U/^{238}U$ is 0.00719 and hence ^{219}Rn is produced in much smaller amounts than ^{222}Rn. ^{220}Rn is short lived relative to ^{222}Rn, so the mean distances of diffusive motion are $0.029m$ for ^{220}Rn and $2.2m$ for ^{222}Rn. ^{222}Rn is by far the dominant nuclide and the most

Table 2.2: Decay series of Actinium (^{235}U)

Isotope	Half life	Decay
^{235}U	$7.1 * 10^{8}y$	α
^{231}Th	$25.5h$	β^-
^{231}Pa	$3.25 * 10^{4}y$	α
^{227}Ac	$21.8y$	β^-
^{227}Th	$18.5d$	α
^{223}Ra	$11.4d$	α
^{219}Rn	$4.0s$	α
^{215}Po	$1.78ms$	α
^{211}Pb	$36.1min$	β^-
^{211}Bi	$2.13min$	α
^{207}Tl	$4.77min$	β^-
^{207}Pb	stable	-

Table 2.3: Decay series of Thorium (^{232}Th)

Isotope	Half life	Decay
^{232}Th	$1.41 * 10^{10}y$	α
^{228}Ra	$5.7y$	β^-
^{228}Ac	$6.13h$	β^-
^{228}Th	$1.91y$	α
^{224}Ra	$3.64d$	α
^{220}Rn	$55s$	α
^{216}Po	$0.158s$	α
^{212}Pb	$10.64h$	β^-
^{212}Bi	$60.5min$	β^-, α
^{212}Po	$3.04 * 10^{-5}s$	α
^{208}Tl	$3.10min$	β^-
^{208}Pb	stable	-

concerned radon isotope in this study [21].

2.6 Source of Radon

Radon is a major pollutant and radon exposure is an international problem. Attention to this problem and the associated health risks has been growing throughout the world and more than 50 countries now have ongoing projects and have

established regulation mandatory [23]. Radon sources are generally from air, soil and water supply.

2.6.1 Radon in Air

Radon moving through soil pore spaces and rock fractures near the surface of the earth usually escapes into the atmosphere. In constructing a house with a basement, a hole is dug, footings are set, and coarse gravel is usually laid down as a base for the basement slab. Then, once the basement walls have been built, the gap between the basement walls and the ground outside is filled with material that often is more permeable than the original ground. This filled gap is called a disturbed zone.

Radon moves into the disturbed zone and the gravel bed underneath from the surrounding soil. The backfill material in the disturbed zone is commonly rocks and soil from the foundation site, which also generate and release radon. The amount of radon in the disturbed zone and gravel bed depends on the amount of uranium present in the rock at the site, the type and permeability of soil surrounding the disturbed zone and underneath the gravel bed, and the soil's moisture content. Outdoor air ranges from less than 0.1 pCi/L to about 30 pCi/L, but it probably averages about 0.2 pCi/L. Radon in indoor air ranges from less that 1 pCi/L to about 3,000 pCi/L, but it probably averages between 1 and 2 pCi/L [24].

2.6.2 Radon in Soil

Radon forms in rocks and soil that contain uranium or thorium. Rocks have generally been thought to be the major source, radon production and migration in soil and bedrock define radon availability, while specific site and construction characteristics control the radon transfer into houses.

Most of the radon in indoor air comes from soil underneath the home. As

uranium breaks down, radon gas forms and seeps into the house. Radon from soil can get into any type of building such as homes, offices, and schools and build up to high levels in the air inside the building [25].

2.6.3 Radon in Water

Radon gas can also dissolve and accumulate in water from underground sources (called ground water), such as wells. When water that contains radon is used in the home for showering, washing dishes, and cooking, radon gas escapes from the water and goes into the air. It is similar to carbonated soda drinks where carbon dioxide is dissolved in the soda and is released when you open the bottle. Some radon also stays in the water.

The radon in water supply poses an inhalation risk and an ingestion risk. Research has shown that the risk of lung cancer from breathing radon in air is much larger than the risk of stomach cancer from swallowing water with radon in it. Most of the risk from radon in water comes from radon released into the air when water is used for showering and other household purposes.

Radon in the home's water is not usually a problem when its source is surface water. A radon in water problem is more likely when its source is ground water, such as a private well or a public water supply system that uses ground water [25].

CHAPTER 3

DATA ACQUISITION

3.1 AlphaGuard Detector

The AlphaGuard radon monitor is a compact portable measuring system for the continuous determination of radon concentration in air, soil and water. In addition to the radon concentration in air, AlphaGuard measures and records also simultaneously ambient temperature (T_a), relative humidity (RH) and atmospheric pressure (P_a) with integrated sensors.

The radon detector of the AlphaGuard is based on a design-optimized pulse ionization chamber. It is suitable for active measurements. AlphaGuard is both suited for short or long term examination inside as well as outdoor. In regular operation the measuring gas gets in diffusion mode via a large surface glass fiber filter into the ionization chamber. Through the glass fiber filter only the gaseous Rn-222 may pass, while the radon progeny products are prevented to enter the ionization chamber. At the same time the filter protects the interior of the chamber from contamination of dusty particles.

The cylindric ionization chamber of the AlphaGuard has an active volume of 0,56 L. Its metallic interior has a potential of +750 V when the instrument is turned on. Along the longitudinal axis the stiff centre electrode is located which lies on a potential of 0 V. The center electrode is connected with the signal input of the highly sensitive preamplifier unit. The worked up measuring signals of the preamplifier unit are transmitted to an electronic network for further digital processing.

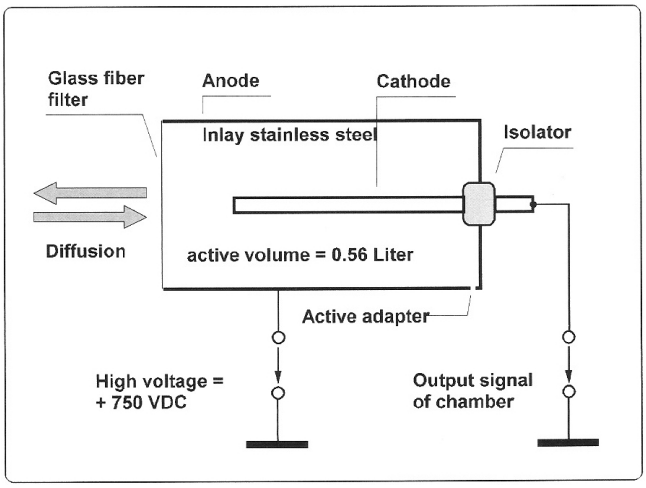

Figure 3.1: AlphaGuard ionization chamber

3.1.1 Digital Signal Processing

For digital signal processing (DSP) there are three independent signal processing channels. To each channel belongs a specific analog-digital converter. This network concept allows analyzing the entering preamplifier signals simultaneously according to three different feature complexes.

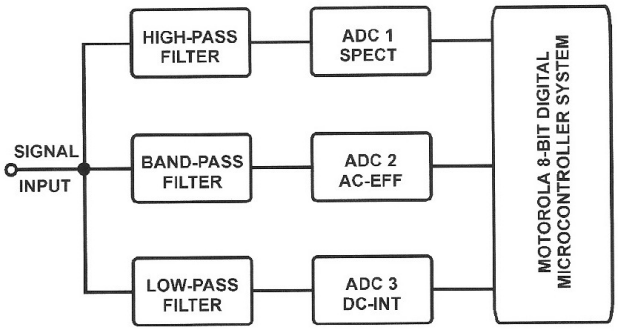

Figure 3.2: The block diagram of digital signal processing

Channel 1 is the spectrometric channel of the AlphaGuard. Here, there is not only a signal characterization according to the pulse depth, but also a classification according to the pulse form. The result of this pulse analysis is a three dimensional spectra. Along the X-axis there is a classification of the pulse depth. By the Y-coordinate the number of pulses per unit of time is described. The

Z-coordinate stands for the classes of pulse forms. Because of this complex pulse characterization a highly effective differentiation between real alpha events and different interference is possible.

In channel 2 signal processing is only affected by high radon concentrations. The dimensioning of the used band pass filter grants that the amplitude of the signal noise level is with high pulse densities direct proportional to the square root of the total ionization stream.

Channel 3 stands for a direct current measurement. Its use is bound to the appearance of extremely high radon concentrations. Moreover it is a guarantee for a high fold back tightness of the measuring system.

On the basis of these three signal characteristics six different analyzing algorithms are processed. Finally, via an optimized density procedure the real radon concentration is determined by them. Any of the displayed radon values of AlphaGuard is the result of 50.000.000 arithmetic operations. Only by use of latest semiconductor generation it is possible to keep the energy consumption of the AlphaGuard down to the low level of 3 mA when handling such heaps of figures.

3.2 E-PERM Electret Detector

The E-PERM system consists of four components: (1) an electrostatically charged teflon disk which collects ions, called an electret; (2) an ion chamber made of conductive plastic into which an electret can be loaded, (3) a reader to read the surface potential (voltage) of the electret, and (4) software to calculate radon concentrations. These components are needed to make an indoor radon measurement as shown in Figure 3.3.

Figure 3.3: The E-PERM system

3.2.1 The Electrets

The electret used in the E-PERM system is a disk of teflon which has been electrically charged and processed by special procedures so that the charge on the electret remains stable even at high humidity or low/high temperatures [26]. The electret disk is secured in a holder that can be screwed into an E-PERM chamber. The electret produces an electrostatic field within the chamber capable of attracting ions of the opposite sign generated by the decay of radon and its daughter products within the chamber. The surface charge is neutralized by the collection of ions and the surface voltage of the electret decreases in proportion to the radon concentration and the exposure time.

There are different types of electrets with different characteristics, which are identified by different colored labels. Short-term (ST) electrets have a high sensitivity, are used principally for short-term measurements, and are identified by blue labels. Long-term electrets are less sensitive, used principally for long-term measurements, and are identified by red labels. A bar code number printed to the back of the electret holder identifies each electret by a unique serial number.

The electrets come with 700 - 780 volts which allows for 500 usable volts. Electrets have less than 200 V should not be used for measurements because the weaker electrostatic field is not as consistent in collecting the ions efficiently.

3.2.2 The Chambers

When an electret is fitted with the chamber, it is called an electret ion chamber and referred to as an E-PERM. As ions are collected, the surface voltage of the electret decreases in proportion to the radon concentration and the exposure time. The decrease in voltage is measured by using an electret voltage reader, known as a SPER-1 Reader [27].

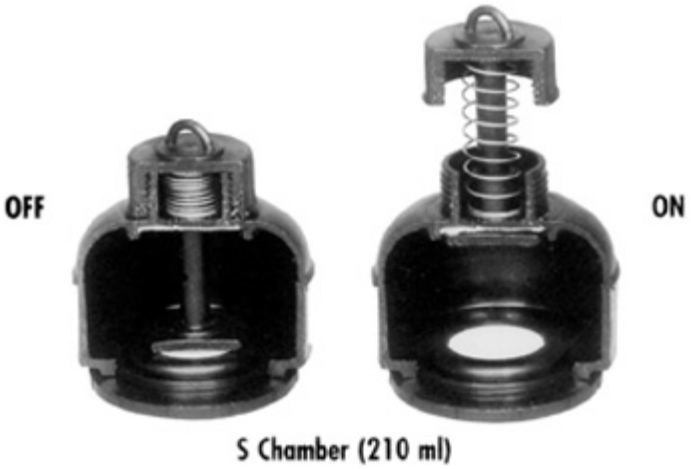

Figure 3.4: Figure of the S Chamber

Radon diffuses into the chamber through filtered openings,the alpha particles emitted by the decay of radon causes ionization, which creates positive and negative ions in the air. When this occurs in the fixed volume of an electrically conducting chamber,the negative ions are drawn towards the surface of the positively charged electret. The electret carries a positive charge and hence collects negative ions from the air, while the positive ions go to the wall of an electrically conducting chamber and are neutralized. The short term chamber is named 'S' which include an on/off mechanism for covering and uncovering the electret. The S Chambers have volume of 210 mL which is used primarily for 2-7 day measurements.

Only radon gas (not the radon progeny present in the air) diffuses through the filtered entry hole into the chamber volume until the concentration of radon

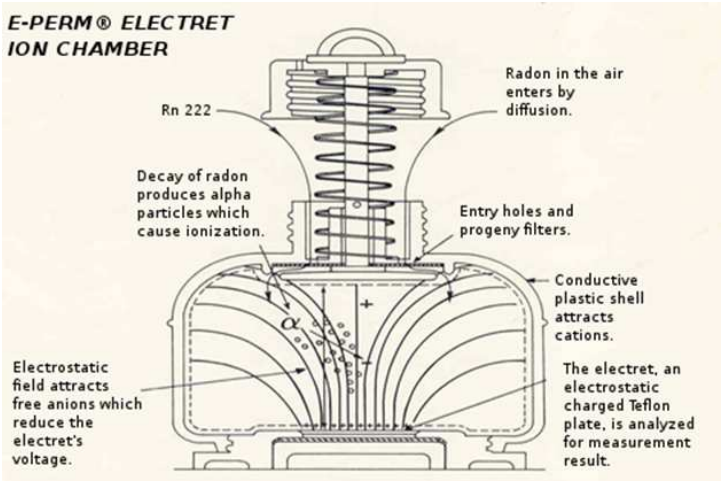

Figure 3.5: The principle operation of an E-PERM electret ion chamber [27]

inside the chamber is the same as that inside the room. Radiation emitted by the decay of radon and the progeny formed inside the chamber ionizes in the air. The positively charged electret attracts the negative ions (anions) generated by the radiation in the chamber resulting in a net decrease of the electret voltage. Positive ions (cations) go to the wall of the chamber and dissipate. The voltage decrease of the electret is proportional to the radon concentration and the time of the exposure. The drop in voltage of the electret is a measure of the product of the radon concentration and the exposure time [28].

3.2.3 The Electret Reader

The SPER (Surface Potential Electret Reader) readers used for measuring the voltage of an electret.The change in the surface voltage of an electret during a known exposure period is a measure of the time-integrated concentration of radon in the E-PERM chamber during that period.

3.3 Measurements and Evaluation

Indoor radon measurements were performed in the Abant Izzet Baysal University, in the northwest part of Turkey, in the Bolu province. Bolu is located between

30°32' - 32°36' east longitude and 40°06'-41°01' north latitude in northwest of Turkey. Bolu is near the capital city of Turkey, with Çankırı locating in eastern, Karabük in northeast, Zonguldak in northern, Düzce in western and Ankara in southern of Bolu. The city is high above sea level about 725 meters and Abant Izzet Baysal University about 900 meters. University campus site is near the North Anatolian Fault Zone (NAFZ) which is a major active right lateral-moving strike-slip fault in northern Anatolia which runs along the transform boundary between the Eurasian Plate and the Anatolian Plate. The NAFZ is totally 1500km in length, 140km and 45km of which were ruptured with the earthquakes (MW 7.4 and 7.2) on August 17, 1999 and November 12, 1999 [29].

In all over the world there are many studies about the radon as precursor of earthquakes. In Japan studies performed by Hatuda (1953), Hirotaka (1988), Igarashi (1995); in India Rastogi (1986), Virk and Singh (1994); Al-Hilal (1998) in Syria, Imme (2005) La Delfa (2007), Morelli (2006) in Italy. Also in Turkey, in soil radon gas was monitored by Friedmann (1988) at the North Anatolian Fault Zone, Bolu. Another study was performed by Baykara and Doğru (2006) and Yalım (2007), for radon measurements in well water, Afyonkarahisar. Radon concentration in thermal water was investigated by Erees (2006, 2007) at two thermal springs, Denizli [30].

Radon concentration levels are strongly affected by geological and geophysical conditions, as well as atmospheric influences such as rainfall and air pressure. Because of the fact that the temperature, rainfall and air pressure are all integrated parts of seasons, so they lead to change in radon concentration levels seasonally. These seasonal variation of radon concentration is also an important area in the environmental physics. So according to Ghosh [31] , radon concentration changes due to meteorological variables such as soil moisture, rainfall, temperature, and air pressure. Also, in the winter season, the radon concentrations are higher than the other seasons. For these reasons, indoor radon measurements were made

in a full year period in order to quantify effect of seasonal conditions on radon concentration.

3.4 Method

Radon measurements were conducted using two different detectors: active ionization detector and passive ionization detector. AlphaGuard is a portable radon monitor which shows radon concentration with integrated sensors. In addition to the radon concentration, AlphaGuard registers simultaneously such ancillary variables as ambient temperature, relative humidity, atmospheric pressure and local time. At the same time radon concentration was measured by using ST-Chamber which is a passive environmental radon monitor. It measures radon and its daughter products. The using detectors are only sensitive for ^{222}Rn measurement. Indoor ^{222}Rn and ancillary variables were measured with both AlphaGuard and ST-Chamber intervals the period May 2012 - May 2013, in the comissaries of five randomly selected faculty buildings: (1) Faculty of Arts and Science (FAS), (2) Faculty of Education (FE) , (3) Faculty of Economics and Administrative Sciences (FEAS) ,(4) School of Foreign Languages (SFL) and (5) School of Physical Education and Sports (SPES) .

First, the radon measurements were performed in the commissaries. The commissaries are located at the basement floor except one which is at second floor of SPES building. Purpose of using two types detector for measurements is to relate active and passive detector with each other. Also with implemented statistical tests, the radon concentration can be correlated with ambient air conditions, location and local time. In the second part, variation of the radon concentration was studied as a function of floor level at FAS building. While all measurements were taken, some important points observed by attention. One of these is the weather condition and seasonal variability. Indoor radon concentration is subject to seasonal variability [32]. A special attention was paid for height and location

of the detector in the medium. AlphaGuard detector was placed on a dining table which is 1m in height and ST-Chambers were hanged from ceiling with 30 cm length sticks. Another important point is the irregular ventilation because both commissaries and office rooms have not special ventilation system. Thus, we usually studied at irregular ventilated (also no smoking) places in all seasons.

CHAPTER 4

ANALYSIS OF DATA

In this chapter, details of the statistical methods and software programs are discussed.

4.1 DataEXPERT Software

DataEXPERT is a professional database and software package for environmental monitoring and analysis. It can be used for data administration and collection as well as for the graphic presentation and documentation of selected measurement series. All the variables can be presented in separate windows or together in one diagram (overlay), and there are convenient zoom functions and mathematical routines for the professional analysis of data, and extensive import as well as export and output options. The data are stored in an integrated database; the system is operable under all current WINDOWS versions.

DataEXPERT can be used for the routine graphic analysis, presentation, and evaluation of measurement data, as well as the storage of the data in the database. DataEXPERT consists of a convenient PC software package with powerful tools. It displays and imports data from dvd files. It selects data from different instruments or measurement series from the database and displays them in one or more windows. It performs powerful zooming, visualizing and mathematical and report functions. Also it exports data easily to Excel, SQL databases [33].

4.2 WinSper Software

WinSper software program has developed by Rad Elec Inc. company for analyzing and generating a Radon Test Report. Although it is easy to use, creates a data

base for tracking electrets, and has QA/QC features. It can remind when the reader or reference electrets need calibration, keep track of the reference electret readings, track individual electrets, and even flag excessive electret voltage loss.

WinSper software has a special calculation for radon concentration. This calculation can be make with manual method, if desired. There is some formulas for it. For calculation of radon concentration, first step is to calculate the Calibration Factor (C_F) :

$$C_F = A + B * ((V_I + V_F)/2) \tag{4.1}$$

In the equation, the A and B calibration constants depend upon the particular E-PERM configuration. The values of A and B constants are 1.69776 and 0.0005742 respectively. The initial and final electret voltage are also used in formula, which written as V_I and V_F.

The second step is calculation of Elevation Correction Factor (E_{CF}) which depends upon the type of chamber being used. The using chamber is Short Term S Chamber; S Chamber Elevation Correction Factor (E_{CF}) in feet is :

If Elevation ≤ 4000 , then $E_{CF} = 1.0$

If Elevation >4000 , then using the following formula:

$$E_{CF} = 0.79 + (6 * Elevation)/100000 \tag{4.2}$$

The last step to calculate radon concentration (C_{Rn}) is :

$$C_{Rn} = \frac{(V_I - V_F) - (0.066667 * D)}{C_F * D} - (BG * G) * E_{CF} \tag{4.3}$$

The radon concentration is in units of pCi/L (equal $37Bq/m^{-3}$), D is the exposure period in units of days, BG is the background gamma which depends on location and G is the gamma conversion constant which is 0.087 for S Chamber.

4.3 Minitab

Minitab is a statistics package which designated mainly as a teaching tool. Although, it is easy to use, it is quite powerful and flexible for moderate size data sets. It was developed at the Pennsylvania State University by researchers Barbara Ryan, Thomas Ryan and Brian Joiner in 1972. Tukey's multiple comparisons following a one-way analysis of variance (ANOVA), two-way ANOVA and regression tests were performed using Minitab 16 (Minitab Inc. State College, PA, USA).

4.3.1 Correlation

Correlation is a measure of the relation between two or more variables. The measurement scales used should be at least interval scales, but other correlation coefficients are available to handle other types of data. Correlation coefficients can range from -1.00 to +1.00. The value of -1.00 represents a perfect negative correlation while a value of +1.00 represents a perfect positive correlation. A value of 0.00 means that there is no linear relationship between the two variables. The most widely-used type of correlation coefficient is Pearson r, also called linear or product moment correlation.

Pearson correlation assumes that the two variables are measured on at least interval scales and it determines the extent to which values of the two variables are "proportional" to each other. The value of correlation (i.e., correlation coefficient) does not depend on the specific measurement units used; for example, the correlation between height and weight will be identical regardless of whether inches and pounds, or centimeters and kilograms are used as measurement units. Proportional means linearly related; that is, the correlation is high if it can be "summarized" by a straight line (sloped upwards or downwards) [34].

4.3.2 Linear Regression

Regression analysis is a statistical technique for investigating and modelling the relationship between variables. Applications of regression are numerous and occur in almost every field, including engineering, the physical and chemical sciences, economics, management, life and biological sciences, and social sciences. In fact, regression analysis may be the most widely used statistical technique [35].

$$y = \beta_0 + \beta_1 x + \epsilon \tag{4.4}$$

The equation is called a linear regression model. The variable x is called the independent or predictor variable and the variable y is called the dependent or response variable. The variable ϵ is a statistical error that is; it is a random variable that accounts for the failure of model to fit the data exactly.

4.3.3 Analysis of Variance

Analysis of Variance, also known as ANOVA is a general method of analyzing data from designed experiments, whose objective is to compare two or more group means [36]. ANOVA was developed by the English statistician, R.A. Fisher (1890-1962). This technique uses tests based on variance ratios to determine whether or not significant differences exist among the means of several groups of observations, where each group follows a normal distribution. The t-test is a special case of ANOVA in which only two means are compared.

4.3.3.1 One-Way ANOVA

The one-way ANOVA is used to compare the means of three or more groups to determine whether they differ significantly from one another. In one-way ANOVA there is one indipendent variable. Its another important function is to estimate the differences between specific groups. The t-test may be thought of as a special

case of one-way ANOVA or it may be regarded as an extension of the t-test to problems involving more than two groups.

There are k groups in one-way ANOVA, where k may be 2 or more. The null hypothesis is that the means are all equal;

$$H_o = \mu_1 = \mu_2 = ... = \mu_k$$

The alternative hypothesis is that at least one of the means is different. We accept the alternative hypothesis H_a , which is that there are at least 2 group means that are significantly different from each other. The alternative hypothesis true when the null hypothesis is false.

4.3.3.2 Two-Way ANOVA

The two-way ANOVA compares the mean differences between groups that have been split on two independent variables (called factors). The primary purpose of a two-way ANOVA is to understand if there is an interaction between the two independent variables on the dependent variable. The two-way ANOVA is an omnibus test statistic and cannot tell which specific groups were significantly different from each other; it only tells that at least two groups were different. Since can be used three, four, five or more groups in the study designs, as well as two independent variables, determining which of these groups differ from each other is important.

4.3.4 General Linear Model

The General Linear Model (GLM) can be used to test almost any hypothesis about a dependent variable that is measured numerically; not categorical variables. There are literally an infinite number of experimental designs and survey designs that can be analysed using the GLM [37].

To measure a response variable Y_j where $j = 1, ..., J$ indexes the observation. Y_j is a random variable, conventionally denoted by a capital letter. Suppose also that for each observation we have a set of L ($L < J$) explanatory variables (each measured without error) denoted by x_{jl} where $l = 1, ..., L$ indexes the explanatory variables. The explanatory variables may be continuous (or sometimes discrete) covariates, function of covariates, or they may be dummy variable indicating the levels of an experimental factor.

A general linear model explains the response variable Y_j in terms of linear combination of the explanatory variables plus an error term :

$$Y_j = x_{j1}\beta_1 + ... + x_{jl}\beta_l + ... + x_{jL}\beta_L + \epsilon_j \tag{4.5}$$

Here the β_l are unknown parameters, corresponding to each of the L explanatory variables x_{jl}. The errors ϵ_j are independent and identically distributed normal random variables with zero mean and variance σ^2.

4.4 Artificial Neural Networks

An artificial neural network is a system based on the operation of biological neural networks, in other words, is an emulation of biological neural system. Numerous advances have been made in developing intelligent systems, some inspired by biological neural networks. Researchers from many scientific disciplines are designing artificial neural networks (ANNs) to solve a variety of problems in pattern recognition, prediction, optimization, associative memory, and control.

A total of 27 ANNs was derived from a combination of 10 different topologies (generalised feed forward-GFF; linear regression-LR; multilayer perceptron-MLP; MLP with principal component analysis-PCA; probabilistic neural network-PNN; radial basis function-RBF; classification support vector machine-SVM; time-delay network-TDNN; recurrent network-RN; and time-lag recurrent network-TLRN),

up to two hidden layers (1 vs. 2), two learning algorithms (Momentum-M vs. Levenberg-Marquardt-L) and two learning modes (batch-B vs. online-O). The ANNs were built using NeuroSolutions 6.01 (NeuroDimension, Inc. Gainesville, FL, USA).

4.4.1 Generalised Feed Forward

Generalized Feedforward Networks (GFFNs) are a special case of multilayer perceptrons such that connections can jump over one or more layers. In theory, a MLP can solve any problem that a GFFN can solve. In practice, however, the GFFNs often solve the problem much more efficiently. The advantage of the GFFN is in its ability to project activities forward by bypassing layers. The result is that the training of the layers closer to the input become much more efficient [38].

4.4.2 Multilayer Perceptron

The most common neural network model is the Multilayer Perceptron (MLP). This type of neural network is known as a supervised network because it requires a desired output in order to learn. The goal of this type of network is to create a model that correctly maps the input to the output using historical data so that the model can then be used to produce the output when the desired output is unknown.

Figure 4.1 shows block diagram of a two hidden layer of MLP. The inputs are fed into the input layer and get multiplied by interconnection weights as they are passed from the input layer to the first hidden layer. Within the first hidden layer, they get summed then processed by a nonlinear function (usually the hyperbolic tangent). As the processed data leaves the first hidden layer, again it gets multiplied by interconnection weights, then summed and processed by the second hidden layer. Finally the data is multiplied by interconnection

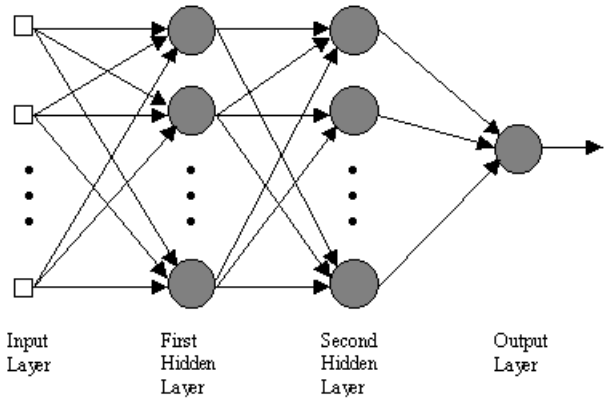

Figure 4.1: A graphical representation of an MLP [39].

weights then processed one last time within the output layer to produce the neural network output [39].

4.4.3 MLP with Principal Component Analysis

Principal Component Analysis (PCA) networks are a mixture of unsupervised and supervised networks. PCA is a linear procedure to find the direction in input space where most of the energy of the input lies. In other words, PCA performs feature extraction. The projections of these components correspond to the eigenvalues of the input covariance matrix. The unsupervised segment of the network performs the feature extraction and the supervised segment of the network performs the (linear or nonlinear) classification of these features using a MLP.

The Principal Component Analysis is performed first, and then the MLP is trained. The reason for this is that the PCA network trains faster when it does not have to share computing resources with the MLP, since there is no point in training the MLP until the eigenvalues are stable.

PCA is a well known method of orthogonalizing data. It converges very fast and the theoretical method is well understood. Since the features are orthogonal, the MLP is able to train easily. There are usually fewer features extracted than

there are inputs, so the unsupervised segment provides a means of data reduction [40].

4.4.4 Probabilistic Neural Network

Probabilistic Neural Network (PNN) is a useful neural network architecture with slightly different in fundamentals from backpropagation. The architecture is feed-forward in nature which is similar to backpropagation, but differs in the way that learning occurs. PNN is supervised learning algorithm but includes no weights in its hidden layer. Instead each hidden node represents an example vector, with the example acting as the weights to that hidden node.

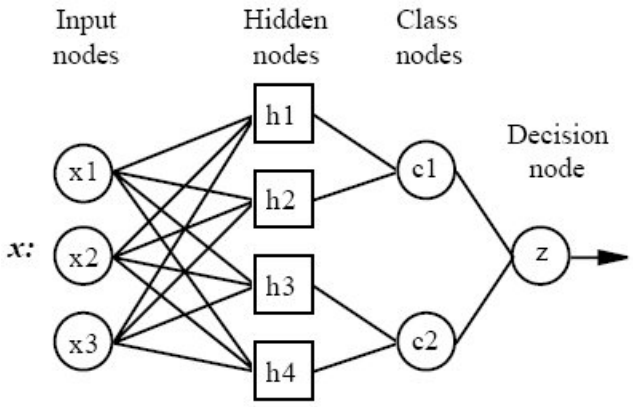

Figure 4.2: A graphical representation of an PNN [41].

Basically, PNN consists of an input layer, which represents the input pattern or feature vector. The input layer is fully interconnected with the hidden layer, which consists of the example vectors (the training set for the PNN). The actual example vector serves as the weights as applied to the input layer. Finally, an output layer represents each of the possible classes for which the input data can be classified. However, the hidden layer is not fully interconnected to the output layer. The example nodes for a given class connect only to that lass's output node and none other [41].

4.4.5 Radial Basis Function

The Radial Basis Function (RBF) network, which has two layers, is a special class of multilayer feed-forward networks. Each unit in the hidden layer employs a radial basis function, such as a Gaussiankernel, as the activation function. The radial basis function (or kernel function) is centered at the point specified by the weight vector associated with the unit. Both the positions and the widths of these kernels must be learned from training patterns. There are usually many fewer kernels in the RBF network than there are training patterns. Each output unit implements a linear combination of these radial basis functions. From the point of view of function approximation, the hidden units provide a set of functions that constitute a basis set for representing input patterns in the space spanned by the hidden units.

RBF networks have a static Gaussian function as the nonlinearity for the hidden layer processing elements. The Gaussian function responds only to a small region of the input space where the Gaussian is centered. The key to a successful implementation of these networks is to find suitable centers for the Gaussian functions. This can be done with supervised learning, but an unsupervised approach usually produces better results. For this reason, NeuroSolutions implements RBF networks as a hybrid supervised-unsupervised topology [42].

4.4.6 Classification Support Vector Machine

Support Vector Machines were introduced by Vladimir Vapnik and colleagues. The earliest mention was in 1979 [43], but the first main paper seems to be 1995 [44]. Support Vector Machines (SVMs) are primarily designed for 2-class classification problems. SVMs were developed to solve the classification problem, but recently they have been extended to the domain of regression problems [44]. They are generally applied using a randomly selected training set classified in advance.

4.4.7 Time-delay Neural Network

Time-Delay Neural Network (TDNN) is an alternative neural network architecture whose primary purpose is to work on continuous data. The advantage of this architecture is to adapt the network online and hence helpful in many applications. The architecture has a continuous input that is delayed and sent as an input to the neural network [45].

4.4.8 Recurrent Neural Network

A neural network is made of individual units termed neurons. Each neuron has a weight associated with each input. A function of the weights and inputs is then generated as an output. Recurrent Neural Networks RNN is a neural network with feedback connections. From training examples RNNs can learn to map input sequences to output sequences. In principle they can implement almost arbitrary sequential behavior. According to Schmidhuber [46], RNNs are biologically more plausible and computationally more powerful than other adaptive models such as feedforward networks and Support Vector Machines.

4.4.9 Time-lag Recurrent Network

Time-Lag Recurrent Networks (TLRNs) are MLPs extended with short term memory structures that have local recurrent connections. The TLRN is a very appropriate model for processing temporal (time-varying) information. Examples of temporal problems include time series prediction, system identification and temporal pattern recognition. The training algorithm used with TLRNs (Backpropagation Through Time) is more advanced than standard Backpropagation.

The main advantage of TLRNs is the smaller network size required to learn temporal problems when compared to MLPs that use extra inputs to represent

the past samples (equivalent to time delay neural networks). An added advantage of TLRNs is their low sensitivity to noise. The recurrence of the TLRN provides the advantage of an adaptive memory depth (i.e., it finds the best duration to represent the input signal's past) [47].

CHAPTER 5

RESULT AND DISCUSSION

Indoor ^{222}Rn and ancillary variables were measured between May 2012 and May 2013 in one day for each month (at 10-min intervals) with AlphaGuard radon monitor and using ST-Chambers as one week for each month in the basements of five randomly selected faculty buildings: (1) Faculty of Arts and Science (FAS), (2) Faculty of Education (FE) , (3) Faculty of Economics and Administrative Sciences (FEAS) , (4) School of Foreign Languages (SFL) and (5) School of Physical Education and Sports (SPES) . In addition, variations in indoor ^{222}Rn concentrations were studied as a function of floor levels (basement and floor levels one to four) and two aspect directions (south and north) at the Faculty of Arts and Science.

Table 5.1: Indoor radon (^{222}Rn) concentration and ambient air condition values of five faculties, measured with AlphaGuard radon monitor.

Variables	Location	n	Mean	SD	Min	Max	Median
^{222}Rn (Bq·m^{-3})	FAS	508	28.5	17.5	2.0	85.0	23.5
	FEAS	379	21.2	11.1	2.0	60.0	20.0
	FE	373	16.9	9.8	0.0	54.0	16.0
	SPES	372	15.9	10.1	0.0	61.0	14.0
	SFL	364	14.0	8.5	0.0	52.0	12.0
T_a(°C)	FAS	508	24.2	1.2	21.1	26.6	24.3
	FEAS	379	22.4	2.5	17.6	28.4	21.9
	FE	373	22.1	1.9	15.2	26.8	21.8
	SPES	372	23.8	1.7	17.8	26.9	24.1
	SFL	364	21.9	2.1	12.6	26.5	22.0
P_a(mbar)	FAS	508	917.9	3.7	909.2	923.8	918.4
	FEAS	379	916.8	5.3	903.6	925.1	916.1
	FE	373	920.2	5.4	907.7	927.8	920.4
	SPES	372	915.5	2.0	911.0	920.4	915.5
	SFL	364	920.9	3.8	915.7	928.9	919.4
RH (%)	FAS	508	37.1	7.9	18.1	54.0	39.5
	FEAS	379	35.5	10.0	15.9	55.3	32.0
	FE	373	38.6	8.6	22.1	59.8	37.5
	SPES	372	30.2	13.7	12.7	60.5	23.3
	SFL	364	32.1	15.2	12.7	59.3	27.4

Mean indoor ^{222}Rn concentrations at the commissaries of the five faculty buildings ranged from 14.0 ± 6.4 Bq·m^{-3} at SFL to 28.5 ± 7.9 Bq·m^{-3} at FAS. Minimum indoor radon concentration observed at both FE, SPES and SFL buildings as zero momentarily. Maximum concentration of indoor ^{222}Rn observed at 10:40 AM in December as 85.0 ± 23.0 Bq·m^{-3} at FAS building; at that moment ambient temperature T_a, atmospheric pressure P_a and relative humidity were 24.0°C, 921.2 mbar and 29.5%, respectively. Maximum indoor radon values of FEAS, FE, SPES and SFL were 60.0 ± 18.0 Bq·m^{-3}, 54.0 ± 16.0 Bq·m^{-3}, 61.0 ± 17.0 Bq·m^{-3} and 52.0 ± 17.0 Bq·m^{-3} respectively as can be seen in Table 5.1. Mean values varied between 21.9 °C at SFL and 24.2 °C at FAS for T_a; between 915.5 mbar at SPES and 920.9 SFL for P_a; and between 30.2% at SPES and 38.6% at FE for RH. All the mean indoor ^{222}Rn concentrations in the five faculty buildings appeared to stay below the world average ^{222}Rn concentration of 40.0 Bq·m^{-3} as reported by UNSCEAR (2000) [48].

Table 5.2: Indoor radon (^{222}Rn) concentration values of five faculties, measured with ST-Chambers.

Location	n	Mean	SD	Min	Max	Median
FAS	12	39.9	8.6	30.5	56.4	37.4
FEAS	12	36.3	8.1	26.4	54.5	33.7
FE	12	32.5	4.8	24.0	39.9	33.1
SPES	12	42.5	8.7	27.8	53.7	41.8
SFL	12	16.5	8.9	2.0	33.6	15.5

Mean indoor ^{222}Rn concentrations at the commissaries of the five faculty buildings during one year period ranged from 16.5 ± 1.4 Bq·m^{-3} at SFL to 42.5 ± 2.9 Bq·m^{-3} at SPES. Minimum and maximum indoor radon concentration observed as 2.0 Bq·m^{-3} and 56.0±3.0 Bq·m^{-3} in November and May at SFL and FAS buildings respectively. Maximum indoor radon values of FEAS, FE, SPES and SFL were 54.5 ± 4.0 Bq·m^{-3}, 39.9 ± 3.0 Bq·m^{-3}, 53.7 ± 4.0 Bq·m^{-3} and 33.6 ± 3.0 Bq·m^{-3} respectively as can be seen in Table 5.2. Mean indoor ^{222}Rn

concentration of SPES building was slightly above the world average radon concentration of 40.0 Bq·m^{-3} [48] but other all mean indoor ^{222}Rn concentrations in the four faculty buildings were below the world average ^{222}Rn concentration of 40.0 Bq·m^{-3} .

Tukey's multiple comparisons following a one-way ANOVA, two-way ANOVA and regression test were performed using statistics methods to determine significant mean differences between indoor ^{222}Rn concentrations and ambient air conditions depending on locations, floor levels and aspect directions. General Linear Model (GLM) was used to perform the two-way ANOVA due to unbalanced observations for all possible combinations of the factor levels (five different floors and two aspect directions).

Table 5.3: Pearson′s correlation matrix of indoor radon (^{222}Rn) concentrations with ambient air conditions.

Variables n=1996	Time (h)	^{222}Rn (Bq·m^{-3})	T_a °C	P_a (mbar)
^{222}Rn (Bq·m^{-3})	0.536***			
T_a(°C)	0.40*	-0.057**		
P_a(mbar)	0.162***	0.091***	-0.220***	
RH (%)	0.185***	0.150***	-0.056**	0.021*
***p<0.001, **p<0.05, *p>0.05				

The indoor radon concentrations of the five faculty buildings; FAS, FEAS, FE, SPES and SFL were measured during one year period with AlphaGuard radon monitor and used for regression test. Mean indoor ^{222}Rn concentration was found to correlate positively with RH, P_a and time and negatively with T_a in Table 5.3. Mean T_a was negatively correlated with P_a. The mean indoor radon concentrations with ambient air conditions are given in Table 5.4 as a result of parameters of pearson′s correlation matrix. Mean indoor radon concentration changes positively ($p < 0.001$) with mean T_a, mean RH and mean P_a with the coefficients

in the regression equation (5.1) (where $p < 0.001$ is the probability of obtaining the null hypothesis as true). The mean indoor radon concentration changes negatively ($p < 0.001$) with location and interaction of mean T_a and mean RH. 20.1% of the dependent variable in the multiple non-linear regression equation can be explain with the explanatory variables ambient temperature, relative humidity, atmospheric pressure, location and interaction of ambient temperature and relative humidity.

$$^{222}Rn = -292 + 1.30T_a + 0.318P_a + 1.53RH - 0.0638T_a * RH - 4.26Location \quad (5.1)$$

Table 5.4: Parameters of Pearson′s correlation matrix of indoor radon (^{222}Rn) concentrations with ambient air conditions.

Predictor	Coef.	SE Coef.	T	P
Constant	-292.06	55.75	-5.24	0.000
Temperature	1.3009	0.3920	3.32	0.001
Pressure	0.31778	0.06015	5.28	0.000
Humidity	1.5334	0.2542	6.03	0.000
T_a* RH	-0.06377	0.01104	-5.78	0.000
Location	-4.2575	0.2055	-20.72	0.000

$S = 12.0475 \quad R - Sq = 20.3\% \quad R - Sq(adj) = 20.1\%$

Table 5.5: Pearson correlation matrix of indoor radon concentrations with location and months.

Variables	^{222}Rn	Location	Month
Location	-0,483***		
Month	0,195*	0,000*	
Location*Month	-0,165*	0,626***	0,705***
***p<0.001, **p<0.05, *p>0.05			

The statistic tests regression and ANOVA were applied to the indoor radon concentration, location, month and interaction of location and month, in order to understand the relationships among these variables. These indoor radon concentrations were measured with ST-Chamber at five different faculty buildings in one year period. Mean indoor radon concentrations were found to correlate positively with month and correlate negatively with location ($p < 0.001$) and interaction of location and month in Table 5.5. The mean indoor radon concentrations with spatial and temporal differences are given in Table 5.6 as a result of parameters of pearson′s correlation matrix. The mean indoor radon concentration changes negatively with location and interaction of location and month and positively with month in the regression equation (5.2). The change on mean indoor radon concentration in the multiple non-linear regression equation can explain with location, month and interaction of location and month as 23.2% .

$$^{222}Rn = 41.2 - 4.02Location + 0.695Month - 0.007Location * Month \quad (5.2)$$

Table 5.6: Parameters of Pearson′s correlation matrix of indoor radon (^{222}Rn) concentrations with spatial and temporal differences.

Predictor	Coef.	SE Coef.	T	P
Constant	41.247	6.804	6.06	0.000
Location	-4.023	2.052	-1.96	0.055
Month	0.6949	0.9245	0.75	0.455
Location * Month	-0.0070	0.2788	-0.03	0.980

$S = 10.5411 \quad R - Sq = 27.1\% \quad R - Sq(adj) = 23.2\%$

Two sets of measurements were carried out at a 10-min interval during October 2011 and January 2012 as a function of floor level (basement to fourth level) and the aspect direction (south vs. north) of the FAS building; which showed that the day-time versus night-time indoor ^{222}Rn concentrations did not significantly

Table 5.7: Multiple comparisons of FAS building as a function of floor level and aspect direction in terms of indoor radon (^{222}Rn) concentration based on Tukey's test.

Floors of FAS	Aspect	n	Mean	SD	CV	Min	Median	Max
Basement^a	North^a	14	83.2	15.5	18.6	51.0	83.5	116.0
	South^b	112	103.6	19.3	18.6	72.0	98.0	164.0
Level 1^a	North^a	15	82.2	21.2	25.8	39.0	86.0	114.0
	South^b	16	103.5	9.9	9.6	90.0	103.0	118.0
Level 2^b	North^a	17	52.7	16.0	30.5	24.0	58.0	74.0
	South^a	15	53.4	15.1	28.4	28.0	58.0	75.0
Level 3^b	North^a	14	55.3	9.0	16.2	41.0	56.5	72.0
	South^a	15	47.4	20.1	42.5	15.0	51.0	86.0
Level 4^c	North^a	16	30.6	11.6	38.0	9.0	31.0	52.0
	South^a	18	37.1	7.6	20.5	27.0	36.0	54.0

differ much despite the mean highest and lowest values of 105 ± 46 Bq·m^{-3} at 16:00 PM ($n = 5$) and 71 ± 37 Bq·m^{-3} at 20:00 PM ($n = 14$), respectively. The mean ^{222}Rn concentrations at different floor level except for the fourth level were above the World Health Organization (WHO) recommended limit of radon concentration of 40 Bq·m^{-3} regardless of aspect direction of the offices, but were below the reference level of 300 Bq·m^{-3} for lung cancer risk [49]. The mean indoor ^{222}Rn concentrations at the lower floors were higher than that at the upper floors which support findings of De Francesco [50]. The mean indoor ^{222}Rn concentrations of 101.3 ± 19.9 Bq·m^{-3} at the basement and 93.2 ± 19.4 Bq·m^{-3} at the first floor were significantly higher than those of the other floors. The mean indoor ^{222}Rn value of the north-facing offices (60.0 ± 24.9 Bq·m^{-3}) was significantly lower than that of the south-facing offices (87.7 ± 31.4 Bq·m^{-3}) ($p < 0.001$). The fact that the basement underneath the south-facing front of the FAS building possesses deep cracks would most likely give rise to a greater diffusion of ^{222}Rn into the south-facing offices than the north-facing ones. At the upper floor levels, the significant difference in ^{222}Rn concentrations between the north- and south-facing offices diminished as seen in Table 5.7.

Table 5.8: Pearson′s correlation matrix of indoor radon (^{222}Rn) concentrations.

Variables (n=252)	^{222}Rn (Bq·m^{-3})	Time (h)	$T_a(°C)$	$P_a(mbar)$	RH (%)	Floor Level
Time (h)	-0.019^{*}					
$T_a(°C)$	0.212^{***}	0.017^{*}				
$P_a(mbar)$	0.575^{***}	-0.033^{*}	0.633^{***}			
RH (%	0.012^{*}	0.026^{*}	-0.258^{***}	-0.069^{*}		
Floor	-0.814^{***}	-0.03^{*}	-0.279^{***}	-0.53^{***}	-0.057^{*}	
Aspect	0.396^{***}	0.022^{*}	0.436^{***}	0.566^{***}	-0.43^{***}	-0.342^{***}
***p >0.05; ***p <0.001;	1: north;	2: south				

The mean indoor ^{222}Rn concentrations significantly correlated positively with T_a, P_a and with the change in aspect direction from north to south; but correlated negatively with the upper floor level ($p < 0.001$) in Table 5.8. The ambient T_a correlated positively with P_a and with a change in aspect direction from north to south; but correlated negatively with RH and with the upper floor levels ($p < 0.001$) . The ambient P_a had negative and positive correlations with the upper floor levels and with the shift in aspect direction from north to south, respectively, whereas RH had a negative correlation with the aspect direction from north to south ($p < 0.001$).

Mean indoor ^{222}Rn concentrations at different floors and aspect direction of the FAS building were found to be above the world average radon concentration of 40 Bq·m^{-3} except at the top floor [2]. The WHO (2009) proposed a reference level of 100 Bq·m^{-3} to minimise health risks due to indoor ^{222}Rn exposure. Thus, the south-facing offices at the basement and first floor of the FAS building have indoor ^{222}Rn concentrations slightly greater than the safe minimum standard by WHO and below the action level (148 Bq·m^{-3}) as recommended by the Environmental Protection Agency (EPA) [51]. Mean indoor ^{222}Rn concentrations obtained in this study in the different faculty buildings and the different floor levels and aspect directions of the FAS building are in close agreement with mean indoor findings reported in the related literature [52, 53]. Higher indoor ^{222}Rn concentrations in the lower floors than the upper floors as found by this study are also supported by reports by Kerry [54] and Virk [55].

Table 5.9: A comparison of 27 artificial neural networks (ANNs) developed as a function of time (h), air temperature (T_a, $^\circ$ C), air pressure (P_a, mbar), relative humidity (RH, %), T_a by RH interaction of five faculty buildings based on performance metrics of training, cross−validation and independent validation

	Training			Cross-validation			Independent validation		
Artificial neural network model	**RMSE**	**r^2(%)**	**MAE**	**RMSE**	**r^2(%)**	**MAE**	**RMSE**	**r^2(%)**	**MAE**
GFF-1-B-L (Generalised Feed forward)	1.8	97.99	1.3	3.0	95.34	1.6	2.3	97.41	1.5
GFF-1-B-M	4.0	90.68	2.3	4.9	87.64	2.7	4.5	90.34	2.6
GFF-1-O-M	2.2	97.35	1.5	3.3	94.57	1.8	2.5	97.13	1.5
LR-0-B-L (Linear Regression)	3.8	91.37	2.0	4.6	88.88	2.4	4.4	90.73	2.3
LR-0-B-M	3.9	91.21	2.1	4.6	88.80	2.4	4.5	90.71	2.4
MLP-1-B-L (Multilayer Perceptron)	2.0	97.63	1.3	2.9	95.62	1.6	2.4	97.27	1.5
MLP-1-B-M	3.4	93.30	2.0	4.3	90.43	2.4	3.9	92.87	2.3
MLP-1-O-M	2.2	97.41	1.5	3.3	94.61	1.9	2.6	96.92	1.6
MLP-2-B-L	2.1	97.62	1.4	3.0	95.21	1.7	2.5	97.09	1.6
MLP-2-B-M	4.5	88.32	3.1	5.2	85.78	3.4	4.9	88.40	3.3
MLP-2-O-M	2.1	97.50	1.4	3.1	94.99	1.7	2.4	97.17	1.5
MLPPCA-1-B-L (MLP with PCA)	**2.2**	**97.08**	**1.4**	**3.2**	**94.65**	**1.7**	**2.6**	**96.71**	**1.5**
MLPPCA-1-B-M	4.3	89.78	2.4	5.1	86.13	2.9	4.9	89.11	2.6
MLPPCA-1-O-M	10.0	46.06	8.1	10.0	53.05	7.8	10.3	52.50	8.4
PNN-0-N-N (Probabilistic Neural Network)	1.4	98.85	1.1	3.8	92.15	2.5	3.4	94.49	2.4
RBF-1-B-L (Radial Basis Function)	9.3	48.98	7.2	8.7	59.61	6.5	9.9	53.19	7.7
RBF-1-B-M	11.7	38.19	8.9	12.0	47.71	9.1	13.0	45.32	9.6
RBF-1-O-M	6.1	78.39	4.4	6.6	77.09	4.7	6.7	78.90	4.7
RN-1-B-L (Recurrent Network)	9.7	48.03	7.8	9.7	54.18	7.7	9.8	55.79	7.9
RN-1-B-M	5.1	86.63	3.6	5.5	84.33	3.8	5.5	87.79	3.8
RN-1-O-M	4.2	89.53	2.7	5.0	86.98	3.0	4.7	89.41	3.0
SVM-0-N-N (Classification SVM)	33.4	26.46	31.4	31.3	34.26	29.3	32.1	39.06	30.0
TDNN-1-B-L (Time-Delay Network)	2.6	96.14	1.7	3.7	93.05	2.2	3.3	94.84	2.1
TDNN-1-B-M	4.4	88.29	3.0	5.4	84.62	3.5	5.0	87.98	3.4
TDNN-1-O-M	1.9	97.96	1.4	3.8	92.40	2.3	2.9	96.04	1.9
TLRN-1-B-L (Time-Lag Recurrent Network)	8.4	58.42	6.0	10.0	45.83	7.0	9.6	56.23	6.8
TLRN-1-B-M	4.1	90.07	2.5	5.1	86.13	3.1	5.0	88.35	3.0
TLRN-1-O-M (Time-Delay Network)	2.5	96.20	1.7	4.0	91.61	2.4	3.5	94.08	2.3

The best performing ANN is designated in bold.

A total of 27 ANNs was derived from a combination of 10 different topologies (generalised feed forward-GFF; linear regression-LR; multilayer perceptron-MLP; MLP with principal component analysis-PCA; probabilistic neural network-PNN; radial basis function-RBF; classification support vector machine-SVM; time-delay network-TDNN; recurrent network-RN; and time-lag recurrent network-TLRN), up to two hidden layers (1 vs. 2), two learning algorithms (Momentum-M vs. Levenberg-Marquardt-L) and two learning modes (batch-B vs. online-O). Three datasets were fed into a total of 27 ANNs to emulate ^{222}Rn concentrations which included as input layers (1): T_a, P_a, RH, T_a*RH (an interaction term between T_a and RH), time and location; (2) location, month, location*month; and (3) T_a, P_a, RH, T_a*RH, time, floor and aspect direction. The entire indoor ^{222}Rn and ancillary dataset was randomly partitioned into training, cross-validation and independent validation datasets with the allocation order of 60%, 15% and 25%, respectively, for 27 ANNs. Accuracy performance metrics used for comparing ANNs were root mean square error (RMSE), mean absolute error (MAE) and coefficient of determination (r^2).

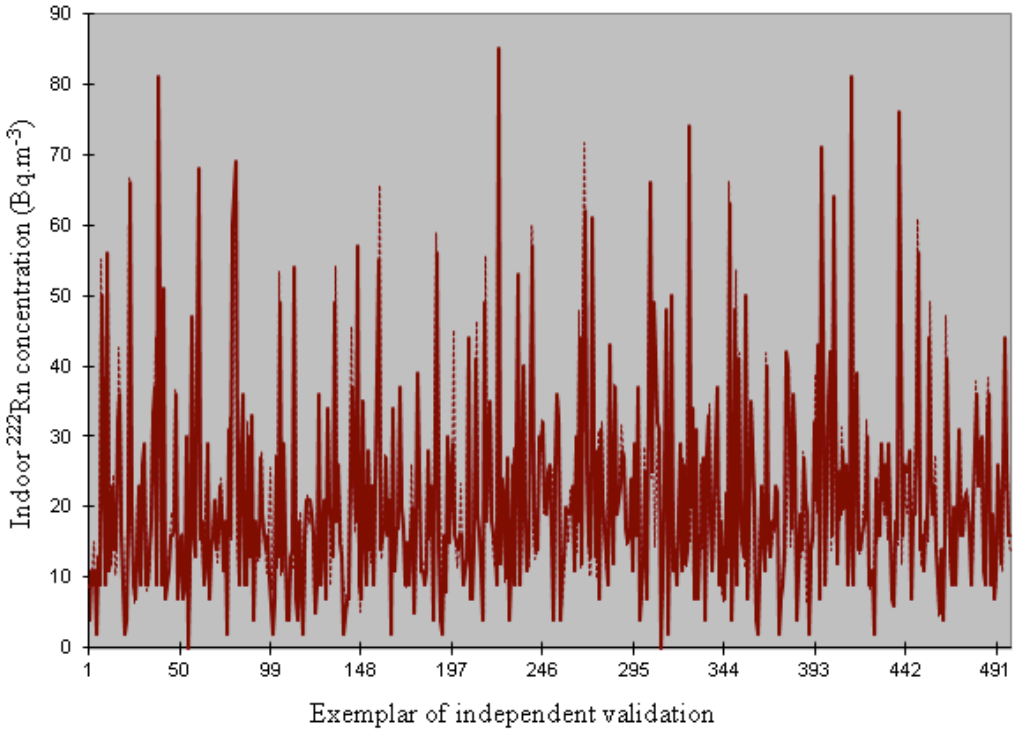

Figure 5.1: Emulations of spatio-temporal dynamics of indoor ^{222}Rn concentrations by the best performing neural networks: MLP with PCA as a function of T_a, P_a, RH, T_a*RH. Solid and discrete lines refer to measured and predicted values of indoor ^{222}Rn, respectively.

The performance metrics derived from training, cross - validation and independent validation of the 27 ANNs indicated that MLP with PCA outperformed best among the other ANNs as a function of T_a, P_a, RH, T_a*RH and time in Table 5.9 and Figure 5.1. The predictive power of the ANNs in terms of r^2 values based on independent validation ranged from 39.1% by SVM-0-N-N to 96.7% by MLP with PCA as a function of T_a, P_a, RH, T_a*RH and time. Independent validation-derived values of r^2, RMSE and MAE pointed to MLP topologies as the best ANNs regardless of the use of plus location.

Table 5.10: A comparison of 27 artificial neural networks (ANNs) developed as a function of month, location, month by location interaction of five faculty buildings based on performance metrics of training, cross−validation and independent validation

	Training			Cross-validation			Independent validation		
Artificial neural network model	**RMSE**	**r²(%)**	**MAE**	**RMSE**	**r²(%)**	**MAE**	**RMSE**	**r²(%)**	**MAE**
GFF-1-B-L (Generalised Feed forward)	5.0	82.78	3.7	3.2	89.82	2.9	14.2	6.90	11.0
GFF-1-B-M	9.8	34.90	8.0	5.3	87.02	3.8	13.8	1.42	11.3
GFF-1-O-M	6.8	70.34	5.7	7.4	73.98	5.7	10.8	46.73	8.0
LR-0-B-L (Linear Regression)	9.8	34.78	7.9	5.8	77.90	4.0	13.8	0.46	11.1
LR-0-B-M	10.4	34.77	7.8	5.4	76.86	3.9	13.4	0.33	10.3
MLP-1-B-L (Multilayer Perceptron)	6.0	75.50	4.8	3.1	90.98	2.9	11.8	29.66	9.0
MLP-1-B-M	10.6	34.34	8.3	4.6	80.01	4.2	15.8	0.00	12.3
MLP-1-O-M	9.4	43.02	8.0	6.8	87.00	5.4	14.8	0.40	12.0
MLP-2-B-L	7.5	62.32	5.5	4.7	82.85	3.9	9.9	53.89	8.0
MLP-2-B-M	9.2	41.44	7.4	5.4	88.67	4.0	13.9	0.51	11.2
MLP-2-O-M	9.4	42.16	7.9	6.4	82.80	4.7	14.7	0.58	11.8
MLPPCA-1-B-L (MLP with PCA)	**7.5**	**61.62**	**6.0**	**4.6**	**78.23**	**3.9**	**9.3**	**59.14**	**7.0**
MLPPCA-1-B-M	11.0	19.90	9.0	6.6	65.44	5.4	11.7	14.53	8.9
MLPPCA-1-O-M	8.5	51.65	7.3	7.7	70.46	6.4	9.5	59.74	7.7
PNN-0-N-N (Probabilistic Neural Network)	1.7	98.31	1.1	6.0	69.60	5.4	10.9	37.82	8.1
RBF-1-B-L (Radial Basis Function)	7.8	57.79	6.8	8.3	43.11	6.7	13.8	2.75	10.6
RBF-1-B-M	8.7	48.91	6.9	5.2	81.07	3.9	15.6	7.84	12.2
RBF-1-O-M	7.6	63.29	6.3	5.2	82.45	3.9	15.7	6.98	12.0
RN-1-B-L (Recurrent Network)	9.5	38.92	7.7	5.2	85.62	3.9	13.8	1.44	11.2
RN-1-B-M	9.8	37.14	7.5	6.3	57.89	5.2	16.6	5.32	13.0
RN-1-O-M	10.0	33.93	8.4	9.8	15.94	6.4	15.7	0.04	13.0
SVM-0-N-N (Classification SVM)	9.9	83.03	7.4	8.9	78.28	6.5	12.6	11.71	9.7
TDNN-1-B-L (Time-Delay Network)	7.3	64.69	5.7	7.7	36.65	5.7	14.5	2.10	12.7
TDNN-1-B-M	7.2	65.25	5.9	4.4	79.5	3.9	15.1	0.80	12.7
TDNN-1-O-M	7.9	58.54	7.1	6.3	70.02	4.8	14.2	5.18	12.1
TLRN-1-B-L (Time-Lag Recurrent Network)	7.7	61.71	6.5	8.5	38.16	6.6	17.7	15.33	14.0
TLRN-1-B-M	5.3	81.84	4.3	6.2	58.15	4.5	15.4	3.06	12.5
TLRN-1-O-M (Time-Delay Network)	5.4	80.98	4.3	6.2	59.74	4.5	15.1	0.85	12.3

The best performing ANN is designated in bold.

The performance metrics derived from training, cross - validation and independent validation of the 27 ANNs indicated that MLP with PCA outperformed best among the other ANNs as a function of month, location, month by location interaction in Table 5.10 and Figure 5.2. The predictive power of the ANNs in terms of r^2 values based on independent validation ranged from 0.0% by MLP-1-B-M to 59.1% by MLP with PCA as a function of location, month and interaction of location and month. Independent validation-derived values of r^2, RMSE and MAE pointed to MLP topologies as the best ANNs regardless of the use of plus location.

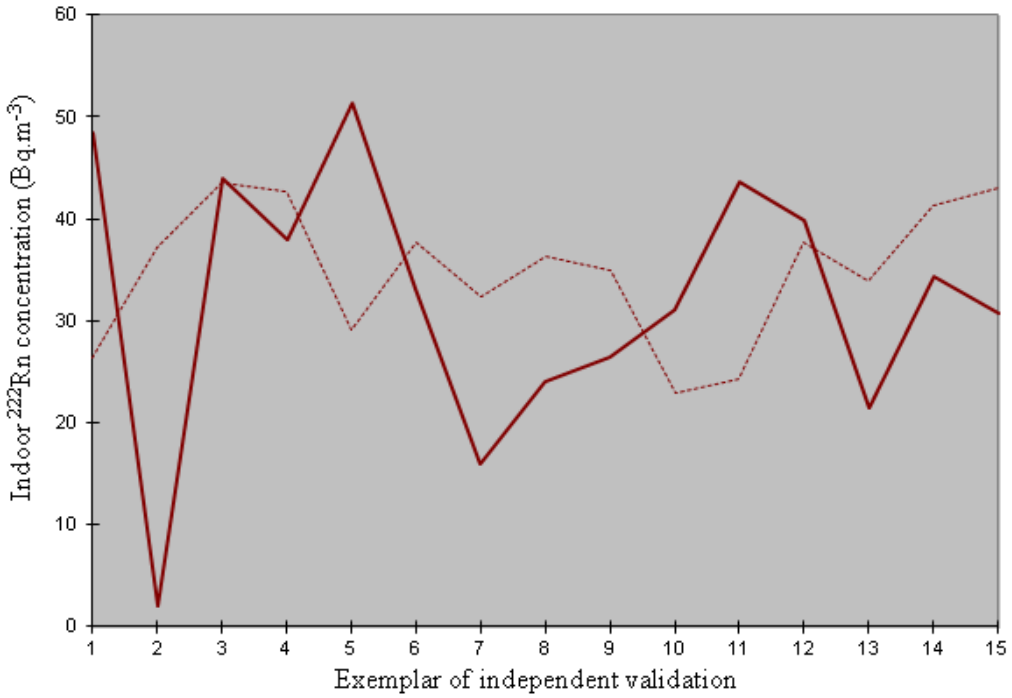

Figure 5.2: Emulations of spatio-temporal dynamics of indoor ^{222}Rn concentrations by the best performing neural networks: MLP with PCA as a function of month, location, month by location interaction. Solid and discrete lines refer to measured and predicted values of indoor ^{222}Rn, respectively.

Table 5.11: A comparison of 27 artificial neural networks (ANNs) developed as a function of time (h), air temperature (T_a, ° C), air pressure (P_a, mbar), relative humidity (RH, %), T_a by RH interaction, floor level and aspect direction of the Faculty of Arts and Science based on performance metrics of training, cross−validation and independent validation

	Training			Cross-validation			Independent validation		
Artificial neural network model	**RMSE**	**r^2(%)**	**MAE**	**RMSE**	**r^2(%)**	**MAE**	**RMSE**	**r^2(%)**	**MAE**
GFF-1-B-L (Generalised Feed forward)	6.9	95.32	4.8	10.9	90.29	8.6	11.2	88.11	8.5
GFF-1-B-M	15.5	76.71	11.8	13.9	83.46	11.5	16.9	71.48	12.9
GFF-1-O-M	11.6	88.25	8.3	12.9	86.12	10.5	13.8	84.33	9.7
LR-0-B-L (Linear Regression)	16.8	72.04	13.0	15.2	80.28	12.3	18.2	66.90	14.3
LR-0-B-M	16.9	71.93	13.1	15.3	80.06	12.4	18.2	67.15	14.3
MLP-1-B-L (Multilayer Perceptron)	8.8	92.43	6.3	10.1	91.14	8.1	11.9	86.04	9.0
MLP-1-B-M	11.4	87.52	8.3	11.7	87.90	9.5	14.0	80.76	10.5
MLP-1-O-M	11.3	88.37	8.2	10.1	91.40	8.3	13.9	83.69	10.1
MLP-2-B-L	**7.5**	**94.52**	**5.6**	**9.9**	**91.42**	**8.0**	**11.1**	**87.62**	**8.9**
MLP-2-B-M	15.2	77.75	11.7	13.6	84.74	11.6	16.8	71.95	12.6
MLP-2-O-M	10.5	89.64	7.3	11.0	89.73	8.8	13.0	84.65	9.0
MLPPCA-1-B-L (MLP with PCA)	35.9	52.96	31.0	37.3	59.15	33.9	36.9	45.44	31.4
MLPPCA-1-B-M	20.8	58.26	16.2	20.2	66.05	17.0	21.2	56.34	16.4
MLPPCA-1-O-M	11.9	86.46	8.9	12.5	86.75	10.4	13.5	82.70	10.0
PNN-0-N-N (Probabilistic Neural Network)	7.5	94.51	4.9	9.8	91.66	7.8	11.5	87.40	8.3
RBF-1-B-L (Radial Basis Function)	15.2	77.21	11.9	14.7	81.56	11.9	16.8	72.67	12.6
RBF-1-B-M	25.0	59.49	19.8	24.4	72.88	20.6	24.7	58.38	18.0
RBF-1-O-M	15.3	77.63	12.0	14.0	84.16	11.4	16.5	73.35	12.7
RN-1-B-L (Recurrent Network)	34.0	31.33	27.6	35.2	36.95	28.7	39.6	15.99	32.4
RN-1-B-M	18.3	68.27	14.3	21.2	65.06	17.3	18.8	67.51	15.5
RN-1-O-M	19.5	65.75	15.9	21.3	64.73	16.7	23.7	50.91	19.2
SVM-0-N-N (Classification SVM)	38.6	75.23	32.6	27.9	67.39	22.5	34.8	55.25	30.0
TDNN-1-B-L (Time-Delay Network)	17.5	71.24	13.1	21.0	65.27	16.8	22.5	50.32	17.9
TDNN-1-B-M	14.1	80.68	10.9	18.2	71.15	14.1	19.9	61.12	16.0
TDNN-1-O-M	17.9	69.10	13.6	19.3	69.90	15.6	24.0	46.75	18.8
TLRN-1-B-M (Time-Lag Recurrent Network)	10.9	88.47	8.2	17.6	72.59	13.6	19.0	64.38	14.5
TLRN-1-O-M (Time-Delay Network)	15.9	81.95	13.4	18.3	71.89	13.8	23.6	59.60	19.4

The best performing ANN is designated in bold.

The performance metrics of FAS building derived from training, cross - validation and independent validation of the 27 ANNs indicated that MLP-2-B-L outperformed best among the other ANNs as a function of T_a, P_a, RH, T_a*RH, time , floor level and aspect direction in Table 5.11. The predictive power of the ANNs in terms of r^2 values based on independent validation ranged from 15.9% by RN-1-B-L to 87.6% by MLP-2-B-L as a function of floor and aspect direction. Independent validation-derived values of r^2, RMSE and MAE pointed to GFF and MLP topologies as the best two ANNs regardless of the use of plus floor and aspect direction.

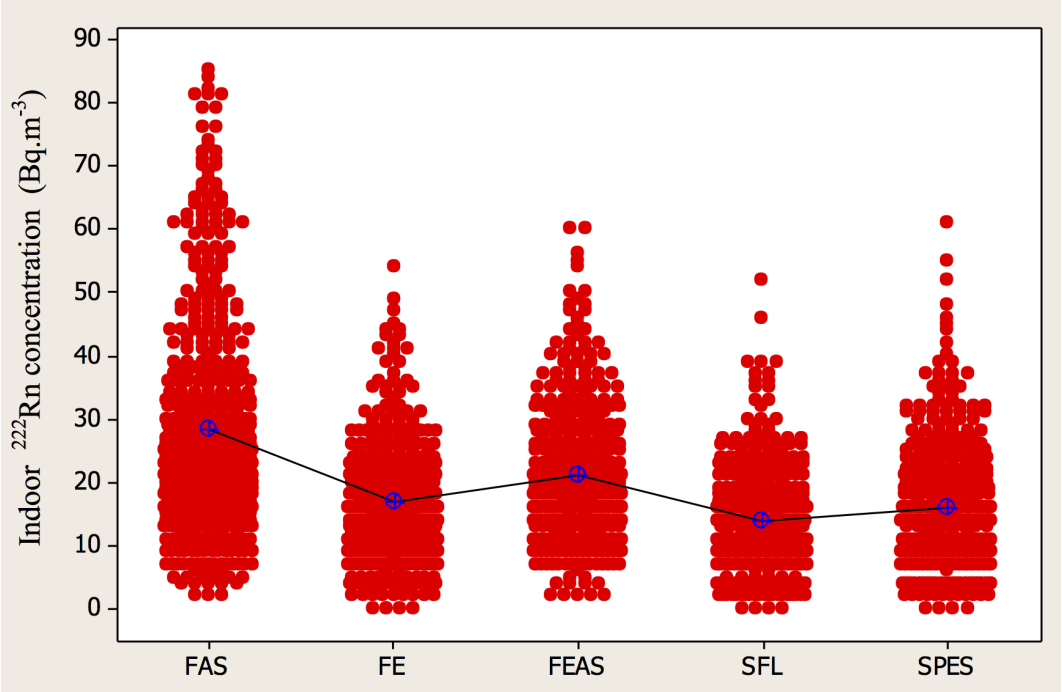

Figure 5.3: Spatial variations in indoor radon (^{222}Rn) concentrations with each months among the faculties of AIBU for AlphaGuard.

Figure 5.3 shows the all indoor ^{222}Rn concentration values measured with AlphaGuard of five faculty buildings for one year period among the locations. Mean indoor ^{222}Rn values was showed with blue points in Figure 5.3. Maximum indoor ^{222}Rn concentrations of FAS, FE, FEAS, SFL, SPES building as 85.0 $\pm$ 23.0 Bq·m^{-3}, 60.0 $\pm$ 20.0 Bq·m^{-3}, 54.0 $\pm$ 16.0 Bq·m^{-3}, 61.0 $\pm$ 17.0 Bq·m^{-3}, 52.0 $\pm$ 17.0 Bq·m^{-3}, respectively. The maximum indoor ^{222}Rn concentration was

measured at FAS. Mean indoor ^{222}Rn concentrations varied between 28.5 ± 8.0 Bq·m^{-3} at FAS, 21.2 ± 8.4 Bq·m^{-3} at FE, 17.0 ± 7.2 Bq·m^{-3} at FEAS, 16.0 ± 7.0 Bq·m^{-3} at SFL and 14.0 ± 6.4 Bq·m^{-3} at SPES. Indoor ^{222}Rn concentrations of faculties of AIBU versus the each months were plotted as in Figure 5.4. Mean indoor ^{222}Rn concentrations of faculties show a low distribution according to UNSCEAR (2000) [48]. Maximum value of mean indoor ^{222}Rn concentration was 26.0 Bq·m^{-3} in September. Also, measured maximum value was 85.0 ± 23.0 Bq·m^{-3} in December at FAS. In winter season the radon concentrations higher than the other seasons [32].

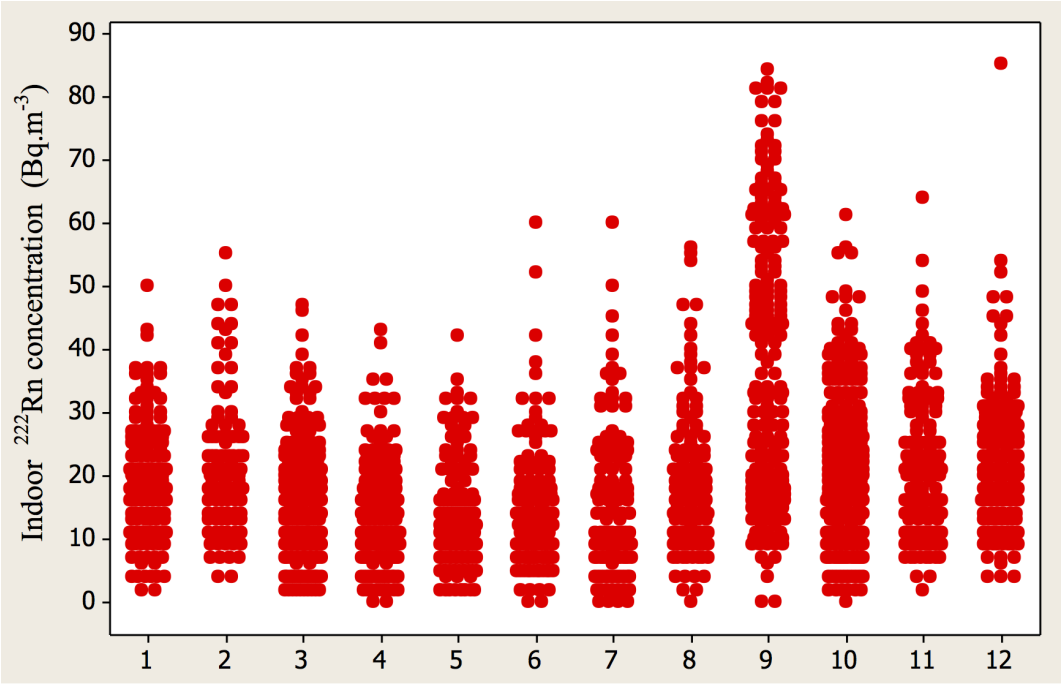

Figure 5.4: Temporal variations in indoor radon (^{222}Rn) concentrations among the each months for AlphaGuard.

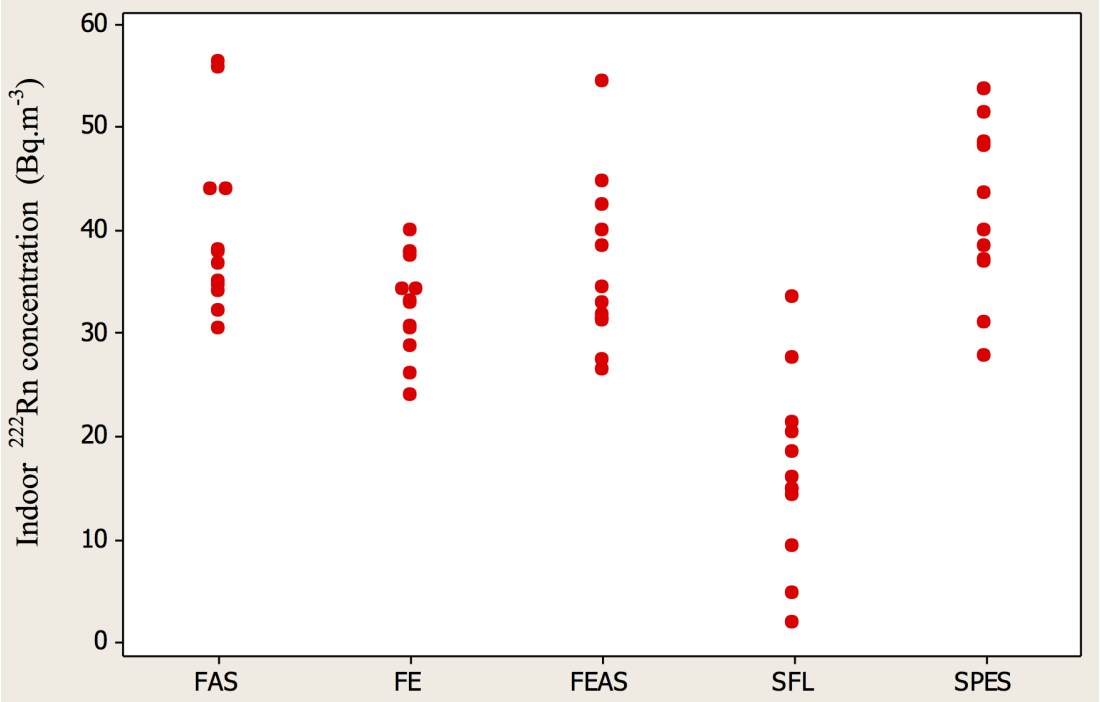

Figure 5.5: Spatial variations in indoor radon (^{222}Rn) concentrations among the faculty locations of AIBU for short term with ST chamber.

Indoor ^{222}Rn concentrations of five faculty buildings versus locations for ST Chamber are shown in Figure 5.5. As can be seen in Figure 5.5, lowest indoor ^{222}Rn concentrations belongs to SFL and mean value of indoor ^{222}Rn was 16.5 $\pm$ 1.4 Bq·m^{-3}. Indoor ^{222}Rn concentration levels were very close in FAS and SPES and maximum mean value of indoor ^{222}Rn was 42.5 $\pm$ 2.9 Bq·m^{-3} at SPES. Indoor ^{222}Rn concentrations of faculties of AIBU versus the each months for short term shown in Figure 5.6. Maximum and minimum mean value of indoor ^{222}Rn concentration were 41.0 $\pm$ 2.7 Bq·m^{-3} in August and 27.9 $\pm$ 2.2 Bq·m^{-3} in April for short term measurement, respectively. Mean indoor ^{222}Rn concentrations in twelve months except for August are below WHO recommended limit of radon concentration of 40 Bq·m^{-3}.

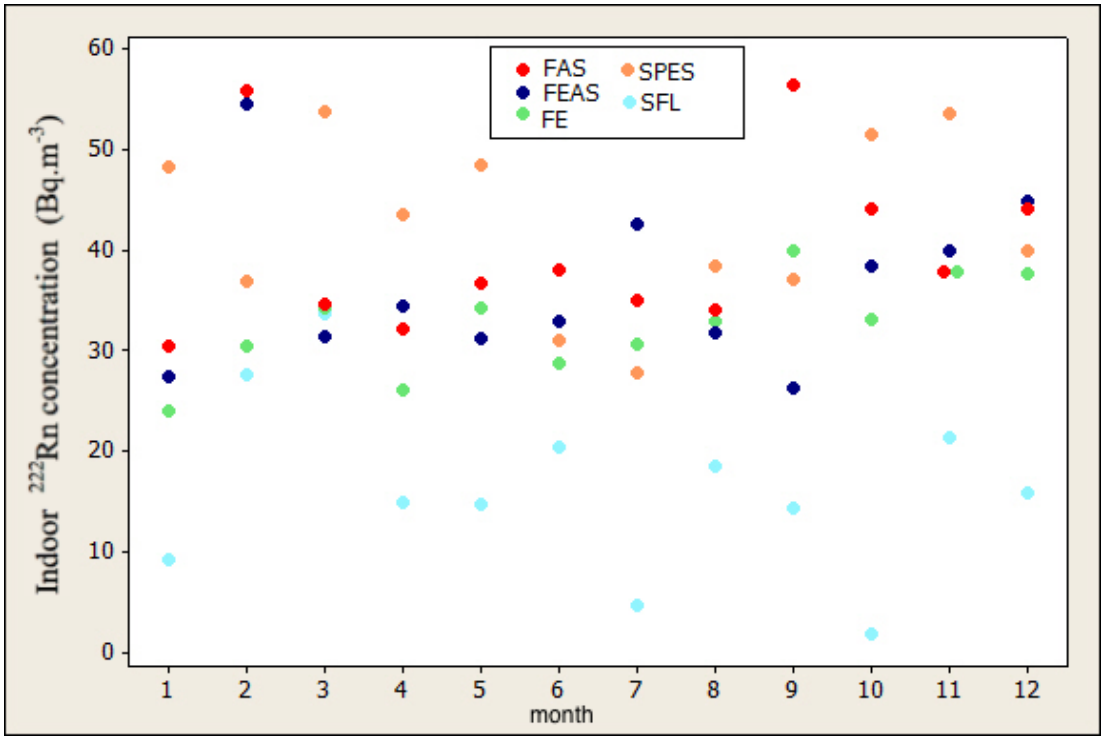

Figure 5.6: Temporal variations in indoor radon (^{222}Rn) concentrations among the months for short term with ST chamber.

The comparison of mean indoor ^{222}Rn concentrations of five faculty buildings of AIBU versus locations for AlphaGuard and ST Chamber are shown in Figure 5.7. The graph has been attributed to the result of study. As can be seen in Figure 5.7, mean indoor ^{222}Rn levels of faculties are compaired for detector types. At FAS, FEAS and FE buildings, mean indoor ^{222}Rn concentration levels for ST-Chamber were greater than mean indoor ^{222}Rn concentration levels for AlphaGuard as nearly 15 Bq·m^{-3} but there was a proximity of mean indoor ^{222}Rn level at SFL for different types of detector. There was a discrepancy between mean indoor ^{222}Rn levels measured with AlphaGuard and ST Chamber at SPES building. Mean indoor ^{222}Rn concentration at SPES was 16.0 Bq·m^{-3} and 42.5 Bq·m^{-3} for AlphaGuard and ST Chamber, respectively. Mean indoor ^{222}Rn concentration levels show consistency for each buildings of AIBU except SPES building.

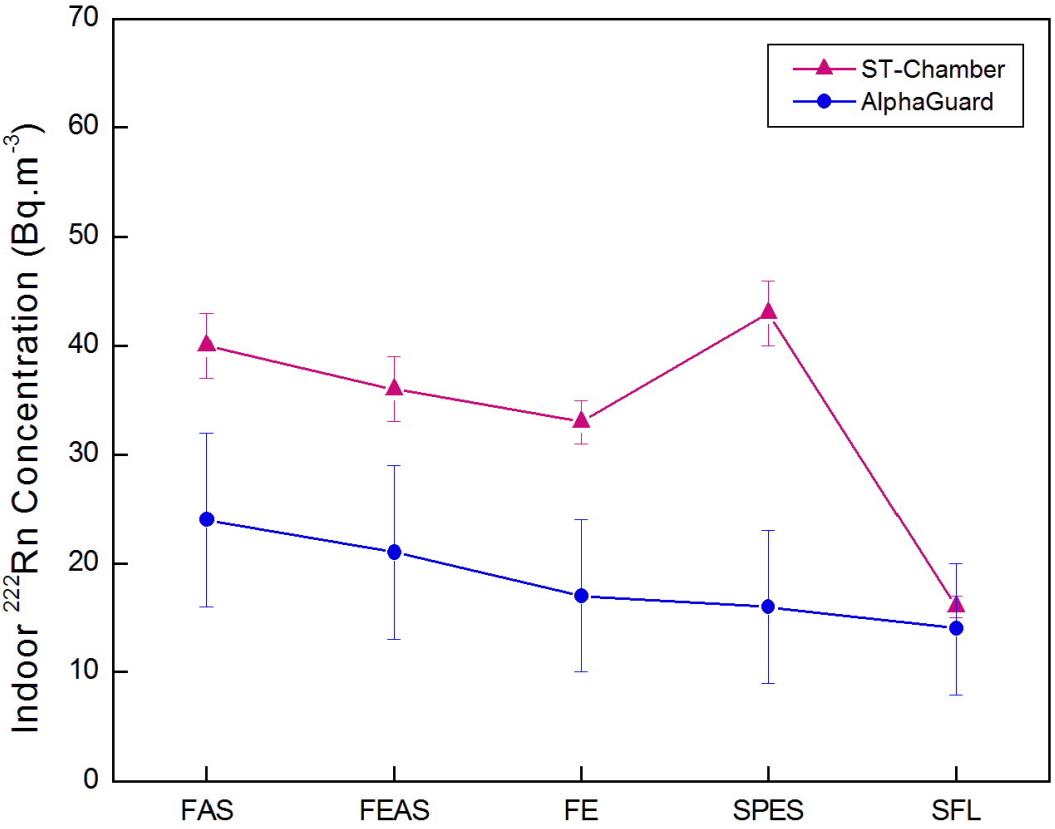

Figure 5.7: Spatial variations in indoor radon (^{222}Rn) concentrations among the faculties of AIBU for two detectors.

CHAPTER 6

CONCLUSION

The present study is the first of its kind to combine a randomised experimental design and 27 ANNs in elucidating spatio-temporal dynamics of indoor ^{222}Rn concentrations. Indoor ^{222}Rn concentrations were found to vary in response to changes in locations at the five faculty buildings of the Abant Izzet Baysal University as well as the interaction effect of the two aspect directions (north and south) and the five different floor levels.

The mean ^{222}Rn concentrations at different floor level except for the fourth level were above 40 Bq·m^{-3} recommended by WHO as limit value of radon concentration at two aspect directions of the offices, but were below the reference level of 300 Bq·m^{-3} for lung cancer risk. Mean indoor ^{222}Rn concentrations at the lower floors were higher than that at the upper floors. According to the Pearson's corellation matrix, mean indoor ^{222}Rn concentrations significantly correlated positively with T_a, P_a and with the change in aspect direction from north to south; but correlated negatively with the upper floor level.In emulating spatio-temporal dynamics of indoor ^{222}Rn levels, the best ANN models of MLP-2-B-L accounted for 87.6% of variations as a function of floor and aspect direction.

The indoor radon concentrations of the five faculty buildings; FAS, FEAS, FE, SPES and SFL which were found to correlate positively with RH, P_a and time and negatively with T_a for AlphaGuard. In emulating spatio-temporal dynamics of indoor ^{222}Rn levels, the best ANN models of MLP with PCA accounted for 96.7% of variations as a function of T_a, P_a, RH, T_a*RH and time.

Mean indoor radon concentrations were found to correlate positively with month and correlate negatively with location and interaction of location and month for ST Chamber. In emulating spatio-temporal dynamics of indoor ^{222}Rn

levels, the best ANN models of MLP with PCA accounted for 59.1% of variations as a function of location, month and interaction of location and month.

Mean indoor ^{222}Rn concentrations of faculties of AIBU for both detectors were below 40 Bq·m^{-3} except mean indoor ^{222}Rn concentration which measured with ST Chamber at SPES building, but all mean indoor ^{222}Rn levels stay below reference level of 100 Bq·m^{-3} to minimise health risks due to indoor ^{222}Rn exposure.

REFERENCES

[1] TAEK, Technical Report 'Indoor Radon Gas: Kapalı Ortamlarda Radon Gazı', March 2012.

[2] Atik S. et al. 'How Do Different Locations, Floors and Aspects Influence Indoor Radon Concentrations? An Empirical Study Using Neural Networks for a University Campus in Northwestern Turkey', Indoor and Built Environment, SAGE, Version of Record August 1, 2013.

[3] Swedjemark G. A. 'An Overview of Radon Indoors' Radiation Protection 98, Scientific Seminar on Radiation Protection in Relation to Radon, 1998.

[4] Hultqvist B., 'Studies on Naturally Occurring Ionizing Radiations,: With special reference to radiation doses in Swedish houses of various types' Kungl. Svenska vetenskapsakademiens handlingar, pp. 76, 1956.

[5] Mjönes L. 'Measurement Protocols for Radon in Dwellings in Sweden;Thirteen Years of Experience' Swedish Radiation Protection Institute, Stockholm, Sweden, April 1993.

[6] *http* : *//www.epa.gov/radon/zonemap.html*

[7] Yücel B. and Arıkan İ.H., 'Binalarda Radon ve Sağlık Etkileri' Standard TSE, Number 531, pp. 108-110, March 2006.

[8] *http* : *//www.epa.gov/radon/pubs/physic.html*

[9] *http* : *//www.ndt−ed.org/EducationResources/HighSchool/Radiography/discoveryxrays.htm*

[10] *http* : *//www.lbl.gov/abc/wallchart/chapters/*03/4.*html*

[11] Michigan State University 'Radiation Safety Manual' Environmental Health and Safety, October 2013.

[12] Proceedings of the International Conference on Non-Ionizing Radiation at UNITEN (ICNIR2003) 'Non-Ionizing Radiations; Sources, Biological Effects, Emissions and Exposures' Electromagnetic Fields and Our Health, $20^{th}-22^{nd}$ October, 2003.

[13] Krane K.S. ' Introductory Nuclear Physics' 2nd Ed., pp. 174-274, 1955.

[14] Magill J. and Galy J. 'Radioactivity, Radionuclides, Radiation' European Commission, Joint Research Centre, Institute for Transuranium Elements, Germany, pp. 44, 2005.

[15] Leo W.R. 'Techniques for Nuclear and Particle Physics Experiments: A How-To Approach' 2nd Rev. Ed., pp. 1-15, 1994.

[16] Mittal V.K. et al., 'Introduction to Nuclear and Particle Physics' New Delhi, pp. 76-141, 2009.

[17] Serway R. and Jewett J. 'Physics for scientists and engineers' Vol.2, 7th Ed., pp. 1081-1082, Printed in USA, 2008.

[18] $https : //www.boundless.com/physics/nuclear - physics - and - radioactivity/gamma - decay/$

[19] Veterans Affairs Palo Alto Health Care System, Stanford University 'Radiation Safety Manual' Environmental Health and Safety, December 2012.

[20] USNRC Technical Training Center 'Radiation Terminology'

$http : //www.nrc.gov/reading - rm/basic - ref/teachers/05.pdf$

[21] Durrani S. A. and Ilic R. 'Radon Measurements by Etched Track Detectors' World Scientific Publication, May 1997.

[22] Agency for Toxic Substances and Disease Registry 'Toxicological profile for radon' U.S. Public Health Service, In collaboration with U.S. Environmental Protection Agency, December 1990.

[23] Ahmed J.U. 'Radon in the human environment: Assessing the Picture' IAEA BULLETIN, pp.32-35, February 1994.

[24] Otton J.K. et al., 'The Geology of Radon' U.S. Geological Survey, 1995. *http : //energy.cr.usgs.gov/radon/georadon.html*

[25] United States Environmental Protection Agency 'Radon in Drinking Water' Office of Water (4607), EPA, October 1999.

[26] Kotrappa P. et al., 'An Electret Passive Environmental 222Rn Monitor Based on Ionization Measurement' Health Phys., Vol. 56, pp. 47-56, January 1988.

[27] *http : //radelec.com//index.php*

[28] Kotrappa P. et al., 'A Practical E-PERM (Electret Passive Environmental Radon Monitor) System for Indoor 222-Rn Measurement' Health Phys., Vol. 58, pp. 461-467, April 1990.

[29] Erdik M. 'Report on 1999 Kocaeli and Duzce (Turkey) Earthquakes' Bogazici University, Dept. of Earthquake Engineering, Istanbul, Turkey

[30] Imme G. and Morelli D., 'Radon as Earthquake Precursor' Earthquake Research and Analysis - Statistical Studies, Observations and Planning, Dr Sebastiano D'Amico (Ed.) In Tech, March 2012.

[31] Ghosh D. et al., 'Anomalous Radon Emission as Precursor of Earthquake' Journal of Applied Geophysics Vol. 69, pp. 67-81, June 2009.

[32] Bossew P. and Lettner H., 'Investigations on indoor radon in Austria, Part 1: Seasonality of indoor radon concentration' Journal of Environmental Radioactivity Vol. 98, pp. 329-345, August 2007.

[33] http://www.saphymo.com/radiation-measurement/environnement /dataexpert/30.htm

[34] $http://www.statsoft.com/$

[35] Montgomery D.C. et al., 'Introduction to Linear Regression Analysis' Wiley Series in Probability and Statistics, 5th Ed., 2013

[36] Bolton S. and Bon C. 'Pharmaceutical Statistics: Practical and Clinical Applications' Drugs and the Pharmaceutical Sciences, Ch. 8, 4th Edition, Vol. 135, December 23, 2009.

[37] Miller J. and Hadden P. 'Statistical Analysis with The General Linear Model' Creative Commons Attribution, Ch. 1, February 16, 2006.

[38] $http://www.nd.com/definitions/genff.htm$

[39] $http://www.neurosolutions.com/products/ns/whatisNN.html$

[40] $http://www.nd.com/models/pca.htm$

[41] Isa K. 'Probabilistic Neural Network (PNN) Algorithm'

$http://urrg.eng.usm.my/$

[42] $http://www.nd.com/models/rbf.htm$

[43] Vapnik V., 'Estimation of Dependences Based on Empirical Data' Moscow, 1979.

[44] Vapnik V., 'The Nature of Statistical Learning Theory' Springer-Verlag, New York, 1995.

[45] Goyal S. and Goyal Kumar G., 'Time-Delay Artificial Neural Network Computing Models for Predicting Shelf Life of Processed Cheese' Broad Research in Artificial Intelligence and Neuroscience, Vol. 3, Issue 1, February 2012.

[46] *http* : *//www.idsia.ch/juergen/oldrnn*4.*html*

[47] *http* : *//www.nd.com/definitions/tlrn.htm*

[48] UNSCEAR (United Nations Scientific Committee on the Effects of Atomic Radiation) 'Sources and Effects of Ionizing Radiation Report to the UN General Assembly with Scientific Annexes 2000' Vienna, Austria, United Nation Scientific Committee on the Effects of Atomic Radiation, 2000.

[49] WHO (World Health Organization) 'Handbook on Indoor Radon' Geneva, Switzerland, 2009.

[50] De Francesco S. et al., Tedesco D. 'Indoor radon seasonal variability at different floors of buildings' Radiation Measurement Vol. 45, pp. 928-934, 2011.

[51] Environmental Protection Agency (EPA) 'A Citizen's Guide to Radon: The Guide to Protecting Yourself and Family from Radon' Washington, DC, 4th Ed., EPA 402-K-02-006, 2005.

[52] Anastasiou T. et al., 'Indoor radon (^{222}Rn) concentration measurements in Cyprus using high-sensitivity portable detectors' Journal of Environmental Radioactivity Vol. 68, pp. 159-169, 2003.

[53] Ojo O.F. et al., 'Determination and evaluation of radiological risk due to indoor radon concentration levels in offices at a University Faculty in Ibadan southwestern Nigeria' Indoor and Built Environment doi:10.1177/1420326X11420586 (in press), 2012.

[54] Kerry A.L. 'Diffusion of radon through cracks in a concrete slab' Health Physics, Vol. 43, pp. 65-71, 1982.

[55] Virk H.S. 'Indoor radon levels near the radioactive sites of Himachal Pradesh, India' Environment International, Vol. 25, pp. 47-51, January 1999.